NASA TECHNICAL MEMORANDUM

NASA TM X-3259

NASA TM X-3259

FLIGHT ASSESSMENT OF A LARGE SUPERSONIC DRONE AIRCRAFT FOR RESEARCH USE

Clinton V. Eckstrom and Ellwood L. Peele

Langley Research Center
Hampton, Va. 23665

NATIONAL AERONAUTICS AND SPACE ADMINISTRATION • WASHINGTON, D. C. • DECEMBER 1975

1. Report No.	2. Government Accession No.	3. Recipient's Catalog No.
NASA TM X-3259		

4. Title and Subtitle	5. Report Date
FLIGHT ASSESSMENT OF A LARGE SUPERSONIC DRONE AIRCRAFT FOR RESEARCH USE	December 1975
	6. Performing Organization Code

7. Author(s)	8. Performing Organization Report No.
Clinton V. Eckstrom and Ellwood L. Peele	L-10333
	10. Work Unit No. 505-02-22-01

9. Performing Organization Name and Address	11. Contract or Grant No.
NASA Langley Research Center Hampton, Va. 23665	

12. Sponsoring Agency Name and Address	13. Type of Report and Period Covered
National Aeronautics and Space Administration Washington, D.C. 20546	Technical Memorandum
	14. Sponsoring Agency Code

15. Supplementary Notes

16. Abstract

An assessment is made of the capabilities of the BQM-34E supersonic drone aircraft as a test bed research vehicle. This assessment is made based on a flight conducted for the purpose of obtaining flight-test measurements of wing loads at various maneuver flight conditions. Flight plan preparation, flight simulation, and conduct of the flight test are discussed along with a presentation of the test data obtained and an evaluation of how closely the flight test followed the test plan.

17. Key Words (Suggested by Author(s))	18. Distribution Statement
Drones Flight operations	Unclassified – Unlimited Subject Category 05

19. Security Classif. (of this report)	20. Security Classif. (of this page)	21. No. of Pages	22. Price*
Unclassified	Unclassified	55	$4.25

*For sale by the National Technical Information Service, Springfield, Virginia 22161

FLIGHT ASSESSMENT OF A LARGE SUPERSONIC DRONE AIRCRAFT FOR RESEARCH USE

Clinton V. Eckstrom and Ellwood L. Peele
Langley Research Center

SUMMARY

Drone-type aircraft are being used by NASA as free-flight research vehicles for the measurement of steady and unsteady loads on aircraft structures and/or active control systems. A flight test was conducted using a BQM-34E supersonic drone aircraft to measure wing loads at various flight-test conditions. This report presents information related to the preparation of a flight plan for and the conduct of such a research flight test in order to evaluate the use of a drone aircraft as a research flight-test vehicle. The flight-test data obtained are discussed along with an evaluation of how closely the flight test followed the flight plan.

INTRODUCTION

Aircraft aerodynamic and structural test data have been obtained over the years through many different techniques, the principal ones being scale-model wind-tunnel tests and full-scale piloted aircraft tests. Recent advances in unmanned, drone-type aircraft offer an additional method of testing with several potential advantages. Specifically, a supersonic target drone-type aircraft is being used by NASA as a free-flight research vehicle for technology advancement, such as the measurement of steady and unsteady loads on experimental aircraft structures and/or active control systems. Of primary consideration is the flight evaluation of different wing planforms and new wing designs as discussed in reference 1. Flight tests of new systems on the drone-type aircraft are an intermediate step between tests of scaled wind-tunnel models and tests on full-scale piloted aircraft. The use of such aircraft is warranted where there is a high risk potential or where lowered costs would result. Many of the initial research efforts planned are focused on the transonic speed range since wind-tunnel testing is especially difficult in this region.

It is anticipated that the primary data to be acquired during the flight tests would be measurements of pressure distributions, local accelerations, and structural loads imposed on the experimental wing and/or control surfaces at specified flight-test conditions. It was desirable therefore to gain experience in conducting such experiments aboard a drone aircraft and to establish the type and quality of data that would be attained from such a flight test.

The drone flight test discussed herein was conducted at the Naval Missile Center, Point Mugu, California. The test vehicle was a standard Navy BQM-34E drone aircraft (supersonic Firebee II) on which NASA had installed four strain gage bridges on the left wing. The purposes of the flight test were: (1) to obtain measurements from the strain gage bridges at several flight loading conditions (vertical load factors ranging from 1g to 5g) from which wing structural loads were to be determined, and (2) to evaluate the capabilities of a drone-aircraft operation (i.e., that it can be utilized to meet the requirements of a prepared flight plan).

The specific flight plan was developed primarily for later use with a standard drone wing instrumented to measure differential pressure distribution on the right wing semispan and structural loads from strain-gage-bridge outputs on the left semispan. For this reason the flight plan included several straight and level steady flight conditions in addition to quasi-steady maneuvers which were used to attain the higher g loading conditions. The straight and level flight runs were for specific Mach number and angle-of-attack conditions. The maneuvers consisted of pull-ups following dives and sustained high g turns. The maneuvers were conducted over a wide range of altitude and angle-of-attack conditions.

The purpose of this report is to document the results of a drone-type flight operation performed for research-flight-testing purposes and to provide an indication of the type and extent of the data obtainable from such a flight test. An evaluation of the experiment to measure wing structural loads is presented in reference 2.

SYMBOLS

Values are given in both SI and U.S. Customary Units. The measurements and calculations were made in U.S. Customary Units.

$\bar{c}$	wing mean aerodynamic chord, 1.195 m (3.92 ft)
C_L	lift coefficient
C_{L_q}	lift coefficient due to rate of change of pitch angle, per degree per second
C_{L_α}	lift coefficient due to angle of attack, per degree
$C^e_{L_\alpha}$	lift coefficient due to angle of attack including effects of aircraft elasticity, per degree
$C_{L_{\dot{\alpha}}}$	lift coefficient due to the rate of change of angle of attack, per degree per second

C_{L_δ}	lift coefficient due to elevon deflection, per degree
C_N	normal-force coefficient
g	acceleration due to gravity, 980 m/sec^2 (32.2 ft/sec^2)
M	Mach number
n_z	normal load factor
q	pitch rate, deg/sec
S	wing gross planform area, m^2 (ft^2)
t	flight time, sec, min, or min:sec
T	thrust, N (lbf)
V	velocity, m/sec (ft/sec)
W	total aircraft weight, N (lbf)
X,Y	Cartesian axes (see fig. 4)
α	angle of attack, deg
α_o	angle of attack at zero lift, deg
$\dot{\alpha}$	rate of change of angle of attack, deg/sec
δ	elevon deflection, deg
ρ	atmospheric density, g/m^3 (slugs/ft^3)
ϕ_c	AFCS commanded aircraft roll angle, deg

FLIGHT-TEST EQUIPMENT

Drone Vehicle

The BQM-34E drone is a turbojet-powered, supersonic, recoverable aircraft developed as a target vehicle for the U.S. Navy. A three-view drawing of the aircraft is shown in figure 1 and an inboard profile is presented as figure 2. The aircraft is capable of flight at a wide range of Mach numbers up to $M = 1.8$ at near maximum altitude and to $M = 1.1$ at sea level as shown in the flight envelope of figure 3. The fuselage-mounted external fuel tank must be jettisoned before beginning supersonic flight.

Instrumented Wing

The left wing of the Navy BQM-34E drone was instrumented with strain gage bridges at four locations as shown in figure 4. A loads calibration was performed where the electrical output of the strain gage bridges was measured for various conditions of shear, bending moment, and torsion loads imposed by the calibrate weights which were applied to various locations on the wing. Load coefficients were then derived by means of a regression analysis for use with measured strain-gage-bridge outputs. It was anticipated that shear, bending moment, and torsion loads in the wing structure could be determined using the load coefficients and the strain-gage-bridge outputs measured during the flight test. Additional information concerning the strain-gage-bridge installations, the loads calibrations, and the derivation of loads equations is presented in reference 2.

Remote Control System

The BQM-34E drone aircraft is controlled during flight from a control center by means of discrete radio command signals sent to an onboard automatic flight control system (AFCS). The AFCS stabilizes the aircraft about the pitch, yaw, and roll axes and provides attitude and flight-path control. A layout of the flight control panel used by the remote control operator (RCO) at the control center is presented as figure 5 which shows the flight control commands available to the RCO. The responses of the drone to the commands of the RCO are generally time-rate controlled by the AFCS; for example, the thrust increases or decreases corresponding to a rate of change of engine speed (rpm) of 1 percent for each second of command time, and the dive and climb commands result in a rate of change of pitch attitude of 1.8° per second of command time. The AFCS also has a minimum allowable engine speed (rpm setting) and maximum allowable dive and climb angles beyond which the vehicle cannot be commanded. To aid in control, the RCO has available radar-track information presented on plotboards and performance data received by telemetry from the drone on strip charts and on a remote indicator panel such as shown in figure 6. A photograph of a typical control center is presented as figure 7.

FLIGHT SIMULATION PROGRAMS

Two different flight simulation programs were used in preparation for the drone-aircraft flight test discussed herein. The first of these was the six-degree-of-freedom digital computer program established by the Naval Missile Center (NMC) and the second was an analog program developed and used by the aircraft manufacturer as a real-time simulator for training purposes.

Digital Flight Simulation Program

The NMC six-degree-of-freedom digital computer program[1] was used to assist in establishing details of the flight plan as will be discussed later. A generalized block diagram of the simulation program is given in figure 8. Note that the flight control system, the aerodynamic forces and moments, the vehicle physical characteristics, and power plant thrust and fuel flow are programed as separate subroutines. Thus, if a new wing and/or control system was used on the drone, the required modifications to the simulation program could be made relatively easily.

The computer simulation program uses each of the flight control commands available to the RCO as command inputs to the simulation program. The program also requires information on the initial flight conditions, the initial vehicle configuration parameters, and the initial control position settings for any given run in addition to several miscellaneous inputs to assure proper processing and presentation of the calculated data.

Analog Flight Simulation Program

The analog simulation program was used to train the RCO for the specific requirements of this flight test using real-time inputs from a flight control panel as was shown in figure 5. Flight information determined by the simulation program was displayed both on strip charts and on a remote indicator panel (fig. 6).

FLIGHT-PLAN PREPARATION

The flight plan selected for this flight test was one which was prepared for flight testing a new drone wing being instrumented by NASA for measurement of differential pressures between the upper and lower wing surface and with strain gage bridges calibrated to provide loads measurements.

---

[1]Programed in FORTRAN for IBM 7090/7094 Direct Coupled System with a conversion for use with CDC 6600 computer system.

For flight testing the new wing, measurements are required at two types of flight condition. One would be a straight and level steady-state flight condition with Mach number and angle of attack as varying parameters. The other type flight condition would be quasi-steady maneuvers to provide a variation of aircraft loading conditions. Although the drone wing flown on the flight test reported herein did not have differential-pressure measuring instruments, a purpose of the flight was to evaluate the capability to achieve each of the flight conditions specified.

For the straight and level steady-state test conditions, the RCO controls the drone flight Mach number by changing the engine speed and therefore the thrust level; however, the angle of attack at which the drone will fly is set by the onboard AFCS as required to maintain level flight. The digital simulation program was used to determine at what altitude the drone would fly at the desired angle of attack for the test condition. An angle of attack of 2° had been selected for the various runs. Priority had been set on attaining test conditions in the transonic speed range and thus Mach numbers of 0.80, 0.85, 0.90, 0.95, 1.06, and 1.10 were selected. The drone aircraft was to cruise for 2 min at an angle of attack of 2° at each of these Mach numbers.

The standard quasi-steady maneuver for attaining symmetrical aircraft loadings with piloted aircraft has been to perform a pull-up maneuver from a diving flight condition. The drone aircraft, however, has safeguards built into the AFCS to prevent abrupt changes in pitch attitude. Therefore the highest loading attainable with a standard AFCS from a pull-up maneuver is on the order of 2g even when the pull-up is initiated from a diving flight condition. Higher loads can be achieved, however, during turning maneuvers. Specifically, if turns are performed below a 4.57-km (15 000-ft) altitude with the AFCS in the "primary-turn" and "altitude-hold" modes, the drone will perform a constant-altitude g-controlled turn at 3g with the external fuel tank on and at 5g with the external fuel tank off. Sustained accelerations of lesser magnitude will result from turns at other flight conditions. Because the wings have no control surfaces (control is by means of elevons) and the turns are "coordinated" (i.e., performed at a constant bank angle and flight altitude – pitch variation is the primary method of altitude control), it was considered that the loading on both wings would be essentially symmetrical and equal to, and therefore similar to, the loads encountered during a pull-up maneuver. Turn maneuvers were therefore included in the flight plan in addition to pull-up maneuvers to achieve the desired range of symmetrical aircraft loading conditions.

Once the test conditions to be included in the flight plan had been established, a rough outline of the test plan was drawn up. The various steps of the flight plan were then simulated using the six-degree-of-freedom digital program mentioned earlier. The digital simulation program was used to assure that the following conditions could be met:

1. That the proposed flight plan allowed sufficient time and fuel for accomplishing the desired flight maneuvers.

2. That the drone-aircraft flight angle of attack would be within $2° \pm 0.2°$ for each of the six cruise conditions.

3. That the proper relationship between flight conditions could be established so that turns could be accomplished to keep the flight within test-range boundaries and that the flight would terminate within the normal recovery area.

4. That most efficient use was made of fuel available in the external fuel tank since it is necessary that the external fuel tank be jettisoned before beginning supersonic flight.

A listing of the flight plan based on the results of the six-degree-of-freedom digital simulation program is presented in table I and a plan view of the proposed flight is presented in figure 9. Using this proposed flight plan, the remote control operators practiced flying the mission in "real time" on an analog simulator to assure that they would be capable of accomplishing the required control tasks within the time, distance, and fuel allotments established. Note that the flight plan listed in table I does not include details associated with the dive and pull-up maneuvers (flight segments 15 to 21). An additional purpose of the RCO practice on the analog simulator was to work out the best sequence for the performance of these maneuvers.

After the successful completion of the practice flights on the analog simulator, the final flight-test-plan document was prepared. This document contained flight-plan listings (including the dive and pull-up maneuvers) and plan views of the proposed flight both for a ground launch of the drone and for an air launch from a P-2V aircraft. These flight-plan listings and plan views are presented as tables II and III and figures 10 and 11, respectively. The most significant difference between the initial flight plan prepared for a ground launch and the final ground-launch flight plan was changing two of the right turns (heading changes of 35° and 90°) to left turns (heading changes of 325° and 270°, respectively) and the addition of a full 360° right turn near the end of the flight. The right turns were changed to left turns to increase the interval of time in the turn during which the aircraft would be in a g-controlled, constant-altitude condition during which symmetrical wing loading would be encountered. The 360° right turn at the end of the flight was added to give at least one turn maneuver that would produce a 5g aircraft loading.

The flight plan developed for the air-launch condition varied somewhat from the ground-launch flight plan primarily because of the different starting point and flight azimuth selected. The longer duration turns came at the second and third turns rather than at the first and second turns as was the case for the ground-launch flight plan. The air-launch flight plan was the one actually used for this flight test.

FLIGHT TEST

The drone vehicle was air launched at a 2.44-km (8000-ft) altitude from a P-2V aircraft. The drone is shown, prior to flight, suspended from the left wing of the P-2V aircraft in figure 12. The drone was launched at 21:25:06.0 GMT and the flight lasted a total of 31 min.

A comparison of the actual flight plan view with the one originally prepared for an air-launch flight test is shown in figure 13. The major differences are the changes in azimuth heading which occurred on the first leg of the flight plan and the downward and outward shifting of the last two legs of the flight plan. The flight-path azimuth change that occurred on the first leg near the end of flight segment number 2 was to avoid aircraft which appeared to be intruding the airspace allotted for the drone flight test. An additional azimuth change was then necessary as the drone approached San Nicolas Island since no drone flights are allowed over any of the inhabited islands in the test range. The shifting of the last two legs of the flight plan was done in an attempt to provide a slightly better position for the final recovery of the drone at the completion of the flight test.

The external fuel pod was jettisoned at 15 min:36.3 sec into the flight test with only 60 N (13.4 lbf) of fuel remaining or 3.35 percent of its capacity. The flight plan had called for the external tank to be released about 1 min later (t = 16 min:35 sec) with about 138 N (31 lbf) of fuel remaining or slightly less than 8 percent of the capacity.

The normal drone recovery sequence was initiated after 30 min:59.2 sec of flight (within 41 sec of when called for in the test plan) when the drone aircraft was at an altitude of 4.1 km (13 500 ft) and a Mach number of 0.92. There were 285 N (64.1 lbf) of fuel remaining in the main fuel tank when the recovery sequence was initiated as compared to the estimate of 111 N (25 lbf) of fuel remaining per the flight plan. (The main fuel tank has a capacity of 1170 N (263 lbf) of fuel.) Initiation of the recovery sequence automatically shut down the engine by cutting off the fuel supply. Because the drone was below a 4.57-km (15 000-ft) altitude and the Mach number was less than 0.94, the AFCS initiated a 16° pitch-up maneuver which resulted in a climb to an altitude of nearly 5.79 km (19 000 ft). The "emergency-chute" command signal was also sent as listed in table IV at 31 min:44.2 sec (45 sec after the "command chute" signal was sent) as a routine backup procedure (no malfunction of the primary chute command was noted). The drag parachute deployed at approximately 31 min:52 sec and the main parachute deployed at approximately 32 min:15 sec for a normal recovery operation. After water impact, a salt-water switch initiated firing of explosive bolts to release the parachute. The recovery helicopter, which was stationed in the recovery area, then picked up the drone and returned it to NMC.

Except for the minor changes mentioned, the flight test was accomplished essentially as planned. A complete listing of all commands sent by the RCO, the time of the commands, and the duration of the commands is presented in table IV.

TEST DATA

Telemetered drone performance data were received on a continuous basis during the flight test. This information was displayed on the RCO display panel (shown in fig. 6) and also recorded on strip charts and magnetic tape. Continuous telemetry data were also received from the four strain gage bridges located on the drone wing. Two FPS-16 radar sets were used to beacon-track the drone aircraft during the flight test. One of these radars was located at Point Mugu and the other was located downrange on San Nicolas Island. Altitude and range-position data from both radars were displayed at the control center during the flight test. The data package provided by the test range included: (1) a digital listing of all the drone performance and strain-gage-bridge measurements telemetered from the drone aircraft, (2) a listing of atmospheric data as measured by a rawinsonde launched 1 hr:35 min after initiation of the drone flight test, and (3) a digital listing of altitude, Mach number, velocity, acceleration, flight-path angle, impact pressure, and dynamic pressure as determined from the FPS-16 radar-track data used in conjunction with the measured atmospheric data.

Mach Number and Altitude Data

A comparison of the Mach number and altitude data as determined by the FPS-16 tracking radar with measurements made onboard the drone aircraft is presented as a function of flight time in figure 14. As can be seen from the figure there is close agreement between the onboard and radar measurements for the entire flight with the exception of three intervals. These are: (1) from 1 to 3 sec flight time when the drone was flying at less than a 1.2-km (4000-ft) altitude, (2) when the drone was flying at or near transonic velocity ($0.98 < M < 1.05$), and (3) near the end of the flight test where the radar-determined Mach number appears to be in error for about 14 sec at the start of the last dive and pull-up maneuver and again for about 50 sec during the 360° 5g right-turn maneuver.

It was noted in the test-range data package that radar tracking data for altitudes below 1.2 km (4000 ft) are extremely unreliable because of the low or negative elevation angles from the tracking radar to the drone target. Therefore during the interval from 1 to 3 sec flight time, when the drone was at less than the referenced altitude, the radar-track data were not considered useful for analysis purposes (at one point during this interval the radar-track data indicated a negative flight altitude). However, when the drone was flying at transonic velocities ($0.98 < M < 1.05$) it is the onboard measurements which are considered to be in error because of the inability of the onboard computer to determine adequately either

Mach number or altitude from pitot-static tube measurements because of shock-wave interference effects. Step changes in the onboard measurements of Mach number and altitude occurred at t = 16 min:30 sec, 17 min:00 sec, 17 min:25 sec, 18 min:20 sec, 18 min:40 sec, 23 min:05 sec, and 23 min:17 sec. No immediate explanation is available for the apparent error in Mach number as determined from radar-track measurements for the intervals from t = 28 min:34 sec to 28 min:48 sec and from t = 29 min:45 sec to 30 min:35 sec. The altitude measurements as determined by the radar data during these intervals are in close agreement with the measurements from onboard the drone aircraft even when the altitude was changing rapidly during the first interval. It is apparent however, that the radar measurements of Mach number are in error and therefore should be excluded from the data analysis during these two time intervals.

Steady-State Cruise Conditions

Figures 15 to 20 present the onboard measurements of flight Mach number and altitude, the drone-aircraft weight as determined from the preflight gross-weight measurement and the onboard measurement of the weight of fuel used, and the onboard measurement of vehicle angle of attack for each of the six straight and level steady-state cruise portions of the flight test. The desired conditions are indicated by the dashed lines and the test points selected for data analysis (table V and ref. 2) are noted by the arrows in each figure.

The first straight and level test run or cruise at M = 0.80 (fig. 15) was delayed while the RCO performed a left-turn maneuver to avoid piloted aircraft intruding into the test range. The desired Mach number was achieved during the second minute of the 2-min interval and the resultant vehicle angle of attack was on the low side, but within the desired angle-of-attack range ($\alpha = 2° \pm 0.2°$). Near the end of this first cruise interval the RCO initiated a second turn to avoid overflying San Nicolas Island and to bring the flight back onto the originally planned areas of the test range.

The second straight and level test run at M = 0.85 (fig. 16) was delayed because of the second unplanned turn just mentioned. The desired flight altitude was achieved at about 50 sec into the test interval. The flight Mach number reached and exceeded the desired value shortly after the flight altitude was achieved and was thereafter slightly higher than planned. The vehicle weight was close to that predicted (within 2 percent) and the resultant angle of attack was at times at the lower boundary (1.8°) of the desired angle-of-attack range. The first planned right turn was initiated at t = 5 min:25 sec, which cut short this second cruise interval. The turn was initiated at this time to maintain proper location on the test range as shown in figure 13.

For the third straight and level test run M = 0.90 (fig. 17) the flight altitude was held constant at about 2.13 km (7000 ft) while the Mach number was increased to the desired value. Even though the flight altitude was slightly lower than planned, and the

vehicle weight was less than anticipated, the resultant angle of attack held steady at 1.8° (the lower edge of the desired range) for about 15 sec (t = 8 min:5 sec to 8 min:20 sec). The increase in altitude at the end of the interval resulted from a climb command initiated to set up for the next test condition.

For the fourth straight and level test run at M = 0.95 (fig. 18) the flight altitude was held at about 4.7 km (15 400 ft) while the Mach number was increased from 0.90 up to a maximum of 0.94 for about 10 sec after which the Mach number dropped back to 0.92. Even though the drone-aircraft weight was less than predicted during this interval and the drone was flying higher and slower than planned, the resultant angle of attack was generally lower than 2° and was only 1.6° to 1.7° (less than the desired lower limit of 1.8°) when the Mach number approached the desired value at t = 10 min:40 sec.

The fifth test run or cruise at M = 1.06 (fig. 19) was performed after the external fuel tank had been released to allow supersonic flight. However during most of the test interval the flight Mach number was in the transonic range ($0.98 < M < 1.05$) where (1) the onboard measurements of Mach number and altitude are known to be in error and (2) the onboard automatic flight control system (AFCS) operates in the transonic mode. When the AFCS is operating in the transonic mode, the drone will fly straight and with the wings level but it will not maintain a constant altitude (i.e., altitude-hold mode is inactive). In this instance the drone aircraft continued to climb slowly throughout the test interval reaching the desired flight altitude at t = 17 min:55 sec based on radar tracking data. Radar-track altitude and Mach number data have been included in figure 19 because of the known inaccuracies in the onboard measurements in the transonic range already mentioned. From about t = 17 min:30 sec to 18 min:15 sec both the onboard and radar measurements of Mach number indicate that the Mach number was close to the desired value. Even though the flight-test conditions of Mach number, altitude, and vehicle weight were very close to the values selected based on the digital drone flight-simulation program, the resulting angle of attack was less than the desired lower limit of 1.8°.

The sixth and last straight and level test run at M = 1.10 (fig. 20) was performed at an altitude about 5 percent higher than planned. In this case the vehicle weight was almost exactly as anticipated and the desired Mach number of 1.10 was achieved at about t = 21 min:30 sec. Even so, the resultant vehicle angle of attack was less (1.4° to 1.7°) than the expected range (2° ± 0.2°) based on the preflight digital simulation program.

Controlled Turn Maneuvers

Figures 21 to 24 present the onboard measurements of flight Mach number, altitude, pitch attitude, roll attitude, angle of attack, and g loading (normal load factor) for each of the four g-controlled turn maneuvers performed during the flight test. A g-controlled turn is performed when the AFCS is in both the altitude-hold and primary-turn-control

modes and the RCO commands either a right or left turn. The drone-aircraft roll angles commanded for both the primary- and secondary-turn schedules are presented in figure 25. Note that the primary-turn schedule is also a function of the drone-aircraft configuration (i.e., external fuel tank on or off). When a g-controlled turn is performed the resultant aircraft loading is

$$n_z = \frac{1}{\cos \phi_c}$$

where ϕ_c is the commanded roll from figure 25. For altitudes below 4.57 km (15 000 ft) the g-controlled turns are performed at a 3g level when the external fuel tank is on and at a 5g load level when the external fuel tank is off.

The first of the four g-controlled turns (fig. 21) was a right turn initiated at t = 5 min:25.3 sec. The right-turn command was followed immediately by a primary-turn-schedule command. Because the AFCS was in the altitude-hold mode and the flight altitude was less than 4.57 km (15 000 ft), the turn was a g-controlled turn performed at the 3g level (the external fuel tank was on at this time). As can be seen from figure 21 the right turn was performed at essentially the 3g level. During the turn the drone-aircraft roll angle changed from 68° to a maximum of about 82° back to a minimum of 64°. The primary right turn resulted in a larger change of direction than was desired so it was followed immediately by a left-turn command. The left turn for azimuth correction was performed according to the secondary-turn schedule which, at this flight altitude calls for a roll angle of 45° (see fig. 25). From t = 5 min:55 sec to 6 min:10 sec (fig. 21) the drone aircraft did maintain a nearly constant roll angle of −45° while the aircraft g loading varied from 1.5g to 1.2g. The AFCS was in the altitude-hold mode during these turns (required for a g-controlled turn) and only slight variations in altitude occurred.

The second of the four g-controlled turns (fig. 22) was a left turn followed by two right turns to the secondary-turn schedule for azimuth correction. The flight altitude was just slightly higher than 4.57 km (15 000 ft), therefore, the g-controlled turn was performed at about the 3g aircraft loading level. The roll angle remained fairly constant at about −75°. Note that as the flight Mach number decreased the angle of attack was increased to maintain the 3g loading.

The third g-controlled turn (fig. 23) was a left turn performed at supersonic velocities ($M \geq 1.05$) after the external fuel tank had been jettisoned. As can be seen from the roll-position curve of figure 23 the AFCS did not latch on to the turn command until the fourth set of left-turn primary-turn-schedule commands was sent. This occurred because the drone aircraft was initially operating in the transonic speed range ($0.96 < M < 1.05$) wherein the AFCS will accept turn commands only for the duration of the command. After the second set of turn commands had been sent the RCO sent a straight and level command

(see table IV at a flight time of 19 min:00.4 sec). This command was accepted by the AFCS because the flight Mach number was now greater than M = 1.05. The AFCS automatically engages the altitude-hold mode 5 sec after the straight and level command is received and then turn commands will latch on when received. The third turn command was sent and released before the 5-sec interval had elapsed and therefore remained in effect only for the duration the command was sent. When the fourth turn command was sent a continuous g-controlled turn was performed at a nearly constant aircraft loading level of 1.9g to 2.0g while the aircraft roll angle varied from −54° to −69°. In this instance the g-controlled portion of the turn was terminated too quickly and an additional left turn at the secondary-turn schedule was necessary to achieve the desired azimuth heading. Note that during this later turn the aircraft roll angle held steady at about −46° while the aircraft loading varied from 1.2g to 1.5g. During the portion of the turn performed at the secondary-turn schedule the flight altitude held fairly constant. This was not the case during the primary-turn-schedule portion of the turn wherein there appears to be some correlation between the aircraft roll angle and the altitude changes.

The fourth and last g-controlled turn (fig. 24) was a full 360° right turn performed specifically to attain aircraft loadings at the 5g level. This turn was performed at a flight altitude of less than 4.57 km (15 000 ft) after the external fuel tank was jettisoned. As can be seen from figure 24 the AFCS was unable to maintain a constant 5g aircraft loading during the turn interval although it is obvious that the aircraft roll angle and angle of attack were being varied in an attempt to maintain both a level flight altitude and a constant 5g aircraft loading condition. The right turn ended at slightly more than a 360° change in heading so a left turn was initiated immediately following the right turn to provide the desired azimuth heading. This left turn was performed to the secondary-turn schedule at an aircraft roll angle of −45°. The flight altitude remained fairly level during both parts of the turn.

Pull-Up Maneuvers

Figure 26 presents the onboard measurements of pitch attitude, angle of attack, and aircraft g loading during the five pull-up maneuvers performed during the flight test which resulted in loads of about 2g.

The flight times in figure 26 can be correlated with those in figure 14 to determine the flight-altitude and Mach number changes which occurred with each of the pull-up maneuvers. The first of the pull-up maneuvers occurred very near the beginning of the flight test when the drone was diving to the first straight and level flight altitude of 0.56 km (1850 ft) from the release altitude of near 2.4 km (8000 ft). The peak loading of 1.9g came as the drone pitched up from a nose-down attitude to a nose-up attitude. Note that it was also at this instant that the maximum angle of attack occurred.

The second pull-up maneuver occurred at about three-fourths of the way through the flight test at the end of a dive from about an 11-km (36 000-ft) altitude down to an altitude of a little over 3.66 km (12 000 ft). During the dive the drone aircraft was flying at a pitch-down position of about 25°. Immediately following the climb command sent at t = 24 min:00.9 sec the pitch attitude decreased at a nearly constant rate. It was in this interval that the maximum loading of 2.1g occurred. This dive maneuver was also followed by a straight and level flight interval so the maximum positive pitch angle reached was about 2.5°.

The first two pull-ups resulted from commands given to achieve other flight conditions whereas the third, fourth, and fifth pull-up maneuvers were performed specifically for the purpose of getting pull-up-maneuver loads. These last pull-ups were therefore performed in nearly the same manner. The test plan called for these dives to be initiated from an altitude of about 3.66 km (12 000 ft), a Mach number of 0.78 to 0.85, and at an engine throttle setting of 83 to 86 percent of full throttle. The dive command was to be held until the Mach number reached a value of 0.93 at which time the dive command was to be released and a climb command initiated. As can be seen from figure 14, the flight Mach number during these dives reached a maximum value of 0.94 for dive 3, 0.95 for dive 4, and 0.94 for dive 5 (based on onboard measurements). Maximum aircraft loadings of 2.0g were experienced on dives 3 and 4 and 1.9g on dive 5.

The wing strain-gage-bridge measurements were evaluated, as reported in reference 2, at 18 points of time during the flight test. The type flight maneuvers being performed at these times and the number of such maneuvers involved in the evaluation were as follows:

steady-state straight and level cruise, six
g-controlled turns, four
pull-ups, five
steady climb, one
dives, two

A listing of the flight times and the relevant telemetered data at these times is presented in table V.

Comparisons of Vertical Force Equilibrium

For each of the test times listed in table V an evaluation was made to determine if the forces along the aircraft body axes were in agreement as defined by the following equation:

$$Wn_z - T \sin 8.33° = C_N \frac{1}{2} \rho V^2 S$$

where

$$C_N = C_{L_\alpha}(\alpha - \alpha_o) + C_{L_\delta}\delta + \frac{\bar{c}}{2V}\left(C_{L_{\dot{\alpha}}}\dot{\alpha} + C_{L_q}q\right)$$

The vehicle weight W was determined from the initial vehicle weight and the onboard measurement of the fuel used. Onboard measurements of the normal load factor n_z were available. The thrust T was determined based on the onboard measurements of engine speed (rpm), Mach number, and flight altitude. Onboard measurements of the vehicle angle of attack were also available. Onboard measurements of altitude and Mach number were used in conjunction with temperature and density measurements from an atmospheric sounding to calculate dynamic pressure. The reference area S for the standard BQM-34E drone-aircraft configuration is 2.97 m^2 (32 ft^2).

Evaluation of the normal-force coefficient C_N was based on the assumption that the aircraft angle of attack would be small and that C_N would therefore be equal to C_L. The lift-slope data C_{L_α} (for a rigid aircraft) were determined based on onboard measurements of flight Mach number. The angle-of-attack data came from onboard measurements as mentioned earlier but the zero-lift angles α_o were determined based on onboard measurements of flight Mach number and the vehicle configuration (i.e., external fuel tank on or off). Unfortunately no flight-test measurements of δ, $\dot{\alpha}$, and q were available to evaluate the remaining terms of the C_N equation. An evaluation was made of the possible relative magnitudes of each of the remaining terms using data obtained from the digital flight-simulation program during preparation of the flight-test plan. From this evaluation it was concluded that C_N was primarily a function of the first term of the equation or

$$C_N = C_{L_\alpha}(\alpha - \alpha_o)$$

The comparison of forces based on the above data and assumptions is presented in figure 27. As can be seen most of the data falls close to the line of agreement except for three data points which are for the 3g and 5g turns. A review of the digital flight-simulation program data for these turns revealed that the elevon deflections δ were slightly negative. Therefore if similar elevon deflections were assumed for the flight test and the $C_{L_\delta}\delta$ term was included in the evaluation, then slightly better agreement would be attained. The contribution of the $C_{L_{\dot{\alpha}}}\dot{\alpha}$ and $C_{L_q}q$ terms, however, appeared to remain negligible.

A rather extensive evaluation was conducted to determine what factors could account for the discrepancy in the data for the high g turns. Because the vane-type angle-of-attack sensor was located on an extended nose boom, consideration was given to the possibility of fuselage deflection at the higher aircraft loadings. Such possible deflection would, however,

be in the nose-down direction which would decrease the measured angle of attack rather than increase it as would be necessary to bring the data closer to the line of agreement. Information was available on the effects of elasticity on the lift performance $C^{e}_{L_{\alpha}}$ for both a trimmed and untrimmed aircraft configuration. Results using these data are presented in figures 28 and 29. Forces measured during the high g turns are much closer to the line of agreement but the remaining data have shifted away from the line of agreement.

It is concluded that for straight and level flight and for maneuvers resulting in aircraft load factors of 2g or less, the lift-slope data for an untrimmed rigid aircraft most adequately describe the test data. For the high g turns the lift-slope data for an untrimmed elastic aircraft best describe the test data.

CONCLUDING REMARKS

A flight test was conducted using a supersonic drone aircraft to measure loads at various flight-test conditions and to evaluate the capabilities of such aircraft as research vehicles. The flight profile flown compared quite well with the plan originally prepared except for deviations required and intentionally made during the flight test. Two-minute intervals included for attaining steady-state cruise conditions proved to be extremely useful in that they allowed the remote control operator (RCO) time to recover from unexpected circumstances and still achieve the test conditions. Also in some instances the RCO had time to make necessary corrections during the test interval.

Errors did occur at times in both the radar-track and onboard measurements of flight conditions but an evaluation of both sets of data allowed the more valid measurement to be determined with reasonable confidence.

The automatic flight control system restraints preclude achieving aircraft load factors of greater than 2g during pull-up maneuvers; however, load factors of up to 5g can be achieved during symmetrical turn maneuvers.

Simulation programs were useful in defining the command sequences for the various flight maneuvers and in determining the time, fuel, and range requirements. However, the angles of attack achieved during the straight and level cruise portions of the flight test were lower than those predicted by the flight-simulation program particularly at the higher Mach numbers.

For straight and level flight and for maneuvers resulting in aircraft load factors of 2g or less, the lift-slope data for an untrimmed rigid aircraft most adequately describe the test

data. For turns where the aircraft load factors were equal to or greater than 3g, the lift-slope data for an untrimmed elastic aircraft best describe the test data.

Langley Research Center
National Aeronautics and Space Administration
Hampton, Va. 23665
August 26, 1975

REFERENCES

1. James, H. A.: Feasibility Study of Modifications to BQM-34E Drone for NASA Research Applications. NASA CR-112323, 1972.

2. Peele, Ellwood L.; and Eckstrom, Clinton V.: Strain-Gage Bridge Calibration and Flight Loads Measurements on a Low-Aspect-Ratio Thin Wing. NASA TN D-7979, 1975.

TABLE I.- INITIAL FLIGHT PLAN PREPARED FOR GROUND LAUNCH

Seg. no.	Flight condition	Percent max. engine speed	Altitude		Mach number	Heading, deg	Time, min:sec		Distance traveled				Fuel used		Fuel remaining		Aircraft weight	
									Increment		Total							
			km	ft			Increment	Total	km	n. mi.	km	n. mi.	N	lbf	N	lbf	N	lbf
	Launch	94	0 to 0.08	0 to 270	0 to 0.32	215	0:04	0:04	----	----	-----	-----	---	---	2860	643	9951	2237
1	Climb	100	0.08 to 0.56	270 to 1850	0.32 to 0.80	↓	0:50	0:54	9.70	5.24	9.70	5.24	133	30	2727	613	9818	2207
2	Cruise	90	0.56	1850	0.80	↓	2:00	2:54	32.37	17.48	42.08	22.72	209	47	2518	566	9609	2160
3	Climb	100	0.56 to 1.26	1850 to 4150	0.80 to 0.85	↓	0:26	3:20	7.46	4.03	49.54	26.75	67	15	2451	551	9542	2145
4	Cruise	91	1.26	4150	0.85	↓	2:20	5:40	39.82	21.50	89.36	48.25	254	57	2197	494	9288	2088
5	Climb	100	1.26 to 2.35	4150 to 7700	0.85 to 0.90	↓	0:35	6:15	10.37	5.60	99.73	53.85	84	19	2113	475	9204	2069
6	Cruise	92	2.35	7700	0.90	↓	2:25	8:40	42.97	23.20	142.70	77.05	267	60	1846	415	8937	2009
7	Right turn	92	2.35	7700	0.90	250	0:10	8:50	3.70	2.00	146.40	79.05	18	4	1828	411	8919	2005
8	Climb	100	2.35 to 3.88	7700 to 12 740	0.90 to 0.95	↓	0:35	9:25	10.56	5.70	156.96	84.75	80	18	1748	393	8839	1987
9	Cruise	94	3.88	12 740	0.95	↓	2:30	11:55	45.56	24.60	202.52	109.35	276	62	1472	331	8563	1925
10	Climb	100	3.88 to 10.06	12 740 to 33 000	0.95 to 0.98	↓	2:50	14:45	49.26	26.60	251.78	135.95	249	56	1223	275	8314	1869
	Pod jettison												53	12	1170	263	7980	1794
11	Right turn	90	10.06	33 000	0.98 to 0.92	340	0:30	15:15	10.19	5.50	261.97	141.45	22	5	1148	258	7958	1789
12	Cruise	91	10.06	33 000	1.06	340	2:40	17:55	50.10	27.05	312.06	168.50	151	34	997	224	7807	1755
13	Right turn	100	10.06	33 000	1.06	70	0:35	18:30	8.33	4.50	320.40	173.00	40	9	957	215	7767	1746
14	Cruise	92	10.36	34 000	1.10	↓	2:30	21:00	48.34	26.10	368.72	199.10	138	31	819	184	7629	1715
15	Dive	80	10.36 to 3.05	34 000 to 10 000	1.10 to 0.80	↓												
16	Dive	80 to 100	3.05 to 0.61	10 000 to 2000	0.80 to 0.95	↓												
17	Pull-up	100	0.61 to 3.05	2000 to 10 000	0.95	↓												
18	Dive	80 to 100	3.05 to 0.61	10 000 to 2000	0.95	↓												
19	Pull-up	100	0.61 to 3.05	2000 to 10 000	0.95	↓												
20	Dive	80 to 100	3.05 to 0.61	10 000 to 2000	0.95	↓												
21	Pull-up	100	0.61 to 3.05	2000 to 10 000	0.95	↓												
22	Recovery																	

TABLE II.- FLIGHT PLAN PREPARED FOR GROUND LAUNCH

Seg. no.	Flight condition	Percent max. engine speed	Altitude		Mach number	Heading, deg	Time, min:sec		Distance traveled				Fuel used		Fuel remaining		Aircraft weight	
									Increment		Total							
			km	ft			Increment	Total	km	n. mi.	km	n. mi.	N	lbf	N	lbf	N	lbf
	Launch	(a)	0	0	0 to 0.30	215	0:04	0:04	---	---	----	----	387	87	2571	578	9844	2213
1	Climb	100	0 to 0.56	0 to 1850	0.30 to 0.80		0:38	0:42	1.19	3.9	1.19	3.9	67	15	2504	563	9777	2198
2	Cruise	86	0.56	1850	0.80		2:00	2:42	5.33	17.5	6.52	21.4	173	39	2331	524	9604	2159
3	Climb	100	0.56 to 1.26	1850 to 4150	0.80 to 0.85		0:24	3:06	1.07	3.5	7.59	24.9	36	8	2295	516	9568	2151
4	Cruise	87	1.26	4150	0.85		2:20	5:26	6.64	21.8	14.23	46.7	213	48	2082	468	9355	2103
5	Climb	100	1.26 to 2.35	4150 to 7700	0.85 to 0.90		0:40	6:06	1.89	6.2	16.12	52.9	49	11	2033	457	9315	2094
6	Cruise	89	2.35	7700	0.90		2:24	8:30	7.08	23.2	23.20	76.1	218	49	1815	408	9097	2045
7	Left turn	92	2.35	7700	0.90	250	1:00	9:30	2.92	9.6	26.12	85.7	107	24	1708	384	8990	2021
8	Climb	100	2.35 to 3.89	7700 to 12 750	0.90 to 0.95		0:40	10:10	1.92	6.3	28.04	92.0	62	14	1646	370	8928	2007
9	Cruise	91	3.89	12 750	0.95		2:30	12:40	7.26	23.8	35.30	115.8	240	54	1406	316	8687	1953
10	Climb	100	3.89 to 10.06	12 750 to 33 000	0.95 to 0.90		2:12	14:52	4.57	15.0	39.87	130.8	196	44	1210	272	8492	1909
	Pod jettison		10.06	33 000	0.90								40	9	1170	263	8162	1835
11	Left turn	85	10.06	33 000	0.90	340	0:53	15:45	2.28	7.5	42.15	138.3	67	15	1103	248	8096	1820
12	Accel.	100	10.06	33 000	0.90 to 1.06	340	0:40	16:25	1.99	6.5	44.14	144.8	44	10	1059	238	8051	1810
13	Cruise	87	10.06	33 000	1.06	340	2:00	18:25	6.09	20.0	50.23	164.8	103	23	956	215	7949	1787
14	Right turn	92	10.06	33 000	1.06	63	0:35	19:00	3.17	10.4	53.40	175.2	40	9	916	206	7909	1778
15	Climb	100	10.06 to 10.36	33 000 to 34 000	1.06 to 1.10		0:25	19:25	1.25	4.1	54.65	179.3	31	7	885	199	7878	1771
16	Cruise	87	10.36	34 000	1.10		2:00	21:25	6.52	21.4	61.17	200.7	102	23	783	176	7775	1748
17	Dive/cruise	80 to 83	10.36 to 3.66	34 000 to 12 000	1.10 to 0.85		2:00	23:25	5.95	19.5	67.12	220.2	89	20	694	156	7687	1728
18	Dive/pull-up	83	3.66 to 1.52	12 000 to 5000	0.85 to 0.95		0:35	24:00	1.83	6.0	68.95	226.2	36	8	658	148	7651	1720
19	Climb/cruise	86 to 86	1.52 to 3.66	5000 to 12 000	0.95 to 0.75		1:00	25:00	2.74	9.0	71.69	235.2	120	27	538	121	7531	1693
20	Dive/pull-up	86	3.66 to 1.52	12 000 to 5000	0.75 to 0.95		0:35	25:35	1.83	6.0	73.52	241.2	35	8	503	113	7495	1685
21	Climb/cruise	86 to 86	1.52 to 3.66	5000 to 12 000	0.95 to 0.78		0:55	26:30	2.74	9.0	76.26	250.2	120	27	383	86	7375	1658
22	Dive/pull-up	86	3.66 to 1.52	12 000 to 5000	0.78 to 0.95		0:35	27:05	1.83	6.0	78.09	256.2	36	8	347	78	7340	1650
23	Climb	100	1.52 to 3.66	5000 to 12 000	0.95 to 0.90		0:20	27:25	0.76	2.5	78.85	258.7	85	19	262	59	7255	1631
24	R. turn/recov.	92.5 to 80	3.66	12 000	0.90	[b]63	0:40	28:05	1.74	5.7	80.59	264.4	71	16	191	43	7064	1588

[a]Value determined by launch conditions.

[b]Calls for a 360° turn.

TABLE III.- FLIGHT PLAN PREPARED FOR AIR LAUNCH

Seg. no.	Flight condition	Percent max. engine speed	Altitude		Mach number	Heading, deg	Time, min:sec		Distance traveled				Fuel used		Fuel remaining		Aircraft weight	
									Increment		Total							
			km	ft			Increment	Total	km	n. mi.	km	n. mi.	N	lbf	N	lbf	N	lbf
	Launch	(a)	2.44	8000	0.35	180	---	0:00	---	---	----	----	222	50	2736	615	10 008	2250
1	Dive		2.44 to 0.56	8000 to 1850	0.35 to 0.80		1:30	1:30	3.05	10.0	3.05	10.0	85	19	2651	596	9 924	2231
2	Cruise	86	0.56	1850	0.80		2:00	3:30	5.33	17.5	8.38	27.5	183	39	2478	557	9 751	2192
3	Climb	100	0.56 to 1.26	1850 to 4150	0.80 to 0.85		0:25	3:55	1.07	3.5	9.45	31.0	36	8	2442	549	9 715	2184
4	Cruise	87	1.26	4150	0.85		2:20	6:15	6.64	21.8	16.09	52.8	213	48	2229	501	9 497	2135
5	Right turn	92	1.26	4150	0.85	256	0:18	6:33	0.67	2.2	16.76	55.0	36	8	2193	493	9 461	2127
6	Climb	100	1.26 to 2.35	4150 to 7700	0.85 to 0.90		0:40	7:13	1.89	6.2	18.65	61.2	49	11	2144	482	9 412	2116
7	Cruise	89	2.35	7700	0.90		2:22	9:35	7.08	23.2	25.73	84.4	218	49	1926	433	9 194	2067
8	Climb	100	2.35 to 3.87	7700 to 12 700	0.90 to 0.95		1:05	10:40	1.92	6.3	27.65	90.7	62	14	1864	419	9 132	2053
9	Cruise	91	3.87	12 700	0.95		2:30	13:10	7.25	23.8	34.90	114.5	240	54	1624	365	8 892	1999
10	Left turn	95	3.87	12 700	0.95	315	1:00	14:10	2.99	9.8	37.89	124.3	121	27	1503	338	8 772	1972
11	Climb	100	3.87 to 10.06	12 700 to 33 000	0.95 to 0.90		2:15	16:25	4.57	15.0	42.46	139.3	195	44	1308	294	8 576	1928
	Pod jettison		10.06	33 000	0.90								138	31	1170	263	8 162	1835
12	Accel.	100	10.06	33 000	0.90 to 1.06		0:35	17:00	1.98	6.5	44.44	145.8	45	10	1125	253	8 118	1825
13	Cruise	87	10.06	33 000	1.06		2:00	19:00	6.10	20.0	50.54	165.8	102	23	1023	230	8 016	1802
14	Accel.	93	10.06	33 000	1.06 to 1.09		0:30	19:30	1.52	5.0	52.06	170.8	31	7	992	223	7 985	1795
15	Left turn	93	10.06	33 000	1.09	60	1:30	21:00	4.57	15.0	56.63	185.8	93	21	899	202	7 891	1774
16	Climb	100	10.06 to 10.36	33 000 to 34 000	1.09 to 1.10		0:25	21:25	1.25	4.1	57.88	189.9	36	7	863	194	7 860	1767
17	Cruise	87	10.36	34 000	1.10		2:00	23:25	6.10	20.0	63.98	209.9	98	23	765	172	7 758	1744
18	Dive/pull-up	80	10.36 to 3.66	34 000 to 12 000	1.10 to 0.85		1:15	24:40	3.96	13.0	67.94	222.9	53	12	712	160	7 704	1732
19	Cruise	83	3.66	12 000	0.85		0:40	25:20	1.98	6.5	69.92	229.4	36	8	676	152	7 669	1724
20	Dive/pull-up	83	3.66 to 1.52	12 000 to 5000	0.85 to 0.95		0:40	26:00	1.88	6.0	71.81	235.6	36	8	640	144	7 633	1716
21	Climb	86	1.52 to 3.66	5000 to 12 000	0.95 to 0.78		0:15	26:15	0.70	2.5	72.51	237.9	88	19	552	124	7 549	1697
22	Cruise	86	3.66	12 000	0.78		0:48	27:03	1.98	6.5	74.49	244.4	32	7	520	117	7 513	1689
23	Dive/pull-up	86	3.66 to 1.52	12 000 to 5000	0.78 to 0.95		0:37	27:40	1.83	6.0	76.32	250.4	35	8	485	109	7 477	1681
24	Climb	86	1.52 to 3.66	5000 to 12 000	0.95 to 0.78		0:15	27:55	0.76	2.5	77.08	252.9	85	19	400	90	7 393	1662
25	Cruise	86	3.66	12 000	0.78		0:48	28:43	1.99	6.5	79.07	259.4	35	8	365	82	7 357	1654
26	Dive/pull-up	86	3.66 to 1.52	12 000 to 5000	0.78 to 0.95		0:37	29:20	1.82	6.0	80.89	265.4	36	8	329	74	7 322	1646
27	Climb	100	1.52 to 3.66	5000 to 12 000	0.95 to 0.90		0:15	29:35	0.77	2.5	81.66	267.9	84	19	245	55	7 237	1627
28	Cruise	85	3.66	12 000	0.90		0:48	30:23	1.98	6.5	83.64	274.4	45	10	200	45	7 193	1617
29	Right turn	92	3.66	12 000	0.90	[b]60	0:42	31:05	1.73	5.7	85.37	280.1	71	16	129	29	7 122	1601
30	Cruise/recov.	80	3.66	12 000	0.90 to 0.80	60	0:35	31:40	1.53	5.0	86.90	285.1	18	4	111	25	7 104	1597

[a]Value determined by launch conditions.

[b]Calls for a 360° turn.

TABLE IV.- REMOTE CONTROL OPERATOR COMMAND RECORD

Flight time, min:sec	Command	Command duration, sec	Flight time, min:sec	Command	Command duration, sec
0:06.3	Time share (sideslip)	0.7	5:13.9	Time share (sideslip)	1.8
0:10.4	Time share (impact pressure)	1.9	5:19.5	Time share (impact pressure)	.3
0:20.5	Right turn	2.3	5:25.3	Right turn	.6
0:33.9	Dive	1.5	5:26.4	Primary-turn schedule	1.3
0:41.4	Dive	3.9	5:39.0	Increase thrust	.4
0:45.5	Right turn	5.5	5:49.9	Straight and level	1.8
0:52.6	Climb	3.3	5:52.9	Left turn	.8
0:57.7	Straight and level	2.7	5:55.0	Cruise/decrease thrust	1.4
1:02.7	Cruise/decrease thrust	4.1	6:01.5	Left turn	.2
1:14.1	Cruise/decrease thrust	1.4	6:08.7	Straight and level	1.5
1:17.3	Cruise/decrease thrust	1.3	6:10.6	Cruise/decrease thrust	1.8
1:23.5	Increase thrust	1.1	6:16.4	Cruise/decrease thrust	.4
1:27.2	Strain gage calibrate	2.2	6:24.4	Climb	.5
1:41.1	Right turn	17.9	6:25.4	Increase thrust	1.9
2:01.4	Straight and level	1.1	6:27.3	Climb	1.1
2:12.0	Increase thrust	1.4	6:28.7	Increase thrust	.8
2:31.3	Increase thrust	1.2	6:33.2	Climb	1.4
3:04.0	Cruise/decrease thrust	.4	6:49.0	Dive	2.2
3:06.1	Cruise/decrease thrust	.4	6:52.9	Dive	.7
3:20.7	Left turn	1.0	7:00.3	Straight and level	2.7
3:55.9	Straight and level	2.5	7:17.8	Cruise/decrease thrust	2.9
4:00.5	Right turn	1.5	7:24.1	Increase thrust	.9
4:03.7	Straight and level	1.1	7:25.7	Increase thrust	.8
4:05.7	Increase thrust	2.0	7:27.1	Increase thrust	1.7
4:08.6	Climb	1.2	7:31.6	Increase thrust	.9
4:11.8	Increase thrust	1.0	7:41.0	Left turn	1.1
4:15.2	Climb	1.6	7:42.9	Straight and level	1.1
4:22.0	Climb	1.8	7:48.8	Time share (sideslip)	1.3
4:27.5	Dive	1.2	7:55.6	Time share (impact pressure)	1.1
4:32.0	Left turn	5.0			
4:43.0	Straight and level	3.0	8:29.5	Climb	4.2
4:58.6	Cruise/decrease thrust	.4	8:34.1	Increase thrust	1.9

TABLE IV.- Continued

Flight time, min:sec	Command	Command duration, sec	Flight time, min:sec	Command	Command duration, sec
8:39.0	Increase thrust	1.5	11:59.3	Primary turn	0.9
8:41.4	Cruise/decrease thrust	.5	12:02.6	Increase thrust	1.5
8:55.4	Time share (oil pressure)	1.3	12:04.4	Increase thrust	1.1
			12:53.6	Straight and level	2.2
9:00.1	Time share (EGT)	1.9	12:56.1	Cruise/decrease thrust	2.3
9:03.5	Cruise/decrease thrust	1.6	13:00.6	Straight and level	1.9
9:09.8	Cruise/decrease thrust	.7	13:13.8	Cruise/decrease thrust	1.1
9:11.9	Dive	4.5	13:07.0	Right turn	.9
9:19.4	Climb	1.8	13:12.8	Straight and level	1.4
9:22.3	Climb	3.1	13:16.3	Right turn	3.3
9:27.7	Straight and level	1.8	13:32.5	Straight and level	3.7
9:31.9	Straight and level	1.3	13:45.9	Increase thrust	1.3
9:44.4	Cruise/decrease thrust	2.5	13:47.4	Subsonic Mach hold	1.0
9:47.3	Cruise/decrease thrust	.5	13:48.5	Increase thrust	4.4
9:53.7	Increase thrust	.8	13:53.2	Increase thrust	1.5
9:55.4	Increase thrust	.8	13:55.2	Increase thrust	.9
10:01.1	Increase thrust	.4	13:58.9	Cruise/decrease thrust	2.1
10:03.4	Increase thrust	1.0	14:01.9	Cruise/decrease thrust	1.0
10:07.1	Increase thrust	.6	14:15.4	Cruise/decrease thrust	1.9
10:13.5	Increase thrust	.9	14:28.5	Increase thrust	1.3
10:20.3	Cruise/decrease thrust	.6	14:38.5	Climb	3.4
10:30.1	Cruise/decrease thrust	1.0	14:42.2	Climb	2.1
10:45.4	Cruise/decrease thrust	.5	14:49.4	Cruise/decrease thrust	1.7
10:52.4	Cruise/decrease thrust	.5	14:59.1	Dive	2.0
10:54.3	Increase thrust	.5	15:05.6	Dive	.9
11:36.0	Time share (impact pressure)	1.3	15:07.8	Dive	1.9
			15:20.4	Straight and level	2.8
11:40.5	Strain gage calibrate	3.4	15:25.0	Cruise/decrease thrust	5.0
11:45.2	Telemetry calibrate	.6	15:30.5	Cruise/decrease thrust	2.3
11:46.5	Telemetry calibrate	.5	15:36.3	External tank jettison	2.6
11:47.9	Telemetry calibrate	.5	15:39.4	Cruise/decrease thrust	.5
11:49.0	Telemetry calibrate	.5	15:40.5	Climb	.7
11:58.4	Left turn	.5	15:41.6	Cruise/decrease thrust	.8

TABLE IV.- Continued

Flight time, min:sec	Command	Command duration, sec	Flight time, min:sec	Command	Command duration, sec
15:42.9	Cruise/decrease thrust	2.0	18:36.9	Increase thrust	2.9
15:50.7	Increase thrust	3.2	18:49.3	Left turn	1.3
15:55.7	Increase thrust	5.2	18:52.0	Primary-turn schedule	3.2
16:02.2	Increase thrust	1.7	18:55.8	Left turn	1.0
16:09.7	Dive	2.8	18:57.0	Primary-turn schedule	1.0
16:13.8	Dive	.7	19:00.4	Straight and level	.6
16:16.2	Dive	1.3	19:01.3	Left turn	2.6
16:21.2	Right turn	4.9	19:05.7	Primary-turn schedule	1.4
16:27.8	Increase thrust	2.8	19:06.5	Left turn	4.5
16:31.3	Cruise/decrease thrust	3.4	19:13.4	Primary-turn schedule	2.1
16:35.4	Cruise/decrease thrust	1.0	19:17.5	Increase thrust	1.1
16:36.5	Straight and level	2.5	19:27.2	Cruise/decrease thrust	3.2
16:41.1	Cruise/decrease thrust	1.1	19:30.7	Cruise/decrease thrust	1.0
16:42.6	Cruise/decrease thrust	1.2	19:32.2	Cruise/decrease thrust	.7
16:44.8	Cruise/decrease thrust	1.0	19:35.3	Increase thrust	.9
16:47.4	Cruise/decrease thrust	.4	19:36.6	Increase thrust	.7
16:50.8	Increase thrust	.6	19:41.1	Increase thrust	.8
16:55.0	Cruise/decrease thrust	.6	19:43.9	Increase thrust	1.8
16:58.4	Increase thrust	.4	19:54.5	Increase thrust	.8
17:00.0	Increase thrust	1.2	20:00.2	Time share (impact pressure)	1.8
17:13.5	Increase thrust	4.5			
17:19.2	Increase thrust	3.8	20:02.5	Increase thrust	2.0
17:23.5	Increase thrust	1.1	20:05.8	Time share (EGT)	.7
17:26.0	Increase thrust	2.1	20:23.7	Straight and level	2.8
17:28.3	Cruise/decrease thrust	4.5	20:31.6	Increase thrust	2.8
17:33.9	Cruise/decrease thrust	1.0	20:37.7	Increase thrust	.8
17:35.2	Cruise/decrease thrust	1.9	20:46.9	Cruise/decrease thrust	4.4
17:46.5	Cruise/decrease thrust	1.0	20:52.9	Left turn	.5
17:48.2	Cruise/decrease thrust	1.0	20:58.1	Cruise/decrease thrust	2.1
17:51.2	Cruise/decrease thrust	.8	21:02.5	Cruise/decrease thrust	1.5
17:53.6	Increase thrust	1.3	21:07.4	Straight and level	2.6
18:24.2	Increase thrust	2.7	21:13.0	Cruise/decrease thrust	2.2
18:34.0	Increase thrust	2.3	21:18.4	Cruise/decrease thrust	.8

TABLE IV.- Continued

Flight time, min:sec	Command	Command duration, sec	Flight time, min:sec	Command	Command duration, sec
21:23.5	Cruise/decrease thrust	2.2	25:18.1	Dive	4.2
21:30.0	Increase thrust	.4	25:22.5	High dive	26.5
21:32.0	Increase thrust	1.0	25:49.0	Climb	7.1
21:54.5	Increase thrust	1.2	26:05.3	Increase thrust	5.7
22:10.6	Time share (sideslip)	1.8	26:12.2	Cruise/decrease thrust	4.6
22:16.2	Time share (impact pressure)	1.0	26:19.7	Subsonic Mach hold	2.0
			26:21.8	Increase thrust	1.7
22:36.6	Increase thrust	1.4	26:36.1	Climb	3.5
22:39.0	Increase thrust	.5	26:40.4	Straight and level	2.6
22:40.2	Cruise/decrease thrust	.8	26:55.9	Dive	4.1
22:41.1	Cruise/decrease thrust	.4	27:00.4	High dive	24.1
22:42.1	Time share (oil pressure)	1.0	27:19.1	Increase thrust	.4
			27:25.0	Climb	8.3
22:49.0	Cruise/decrease thrust	2.3	27:44.0	Subsonic Mach hold	1.2
22:51.4	Cruise/decrease thrust	11.0	28:01.4	Climb	3.6
23:05.6	Dive	5.3	28:08.5	Straight and level	2.9
23:11.0	High dive	49.9	28:19.1	Dive	3.8
23:17.2	Dive	1.8	28:23.2	High dive	6.2
23:19.9	Dive	.6	28:29.5	High dive	17.9
23:33.5	Dive	1.3	28:47.6	Climb	9.5
24:00.9	Climb	7.7	28:59.3	Climb	1.6
24:17.0	Straight and level	3.7	29:02.3	Climb	.9
24:22.4	Straight and level	1.6	29:04.0	Subsonic Mach hold	1.9
24:29.6	Dive	1.8	29:09.6	Right turn	5.3
24:34.6	Straight and level	3.9	29:18.5	Right turn	2.1
24:39.2	Increase thrust	.4	29:22.0	Straight and level	6.1
24:40.1	Cruise/decrease thrust	4.8	29:28.8	Increase thrust	12.6
24:45.0	Cruise/decrease thrust	3.1	29:41.4	Right turn	1.3
24:48.3	Cruise/decrease thrust	1.0	29:45.3	Primary-turn schedule	2.0
25:11.6	Time share (impact pressure)	.7	29:49.0	Cruise/decrease thrust	2.2
			29:51.4	Cruise/decrease thrust	2.5
25:12.9	Time share (oil pressure)	.6	29:57.2	Cruise/decrease thrust	1.0
			30:12.1	Cruise/decrease thrust	1.4

TABLE IV.- Concluded

Flight time, min:sec	Command	Command duration, sec
30:17.1	Increase thrust	1.9
30:24.5	Increase thrust	2.2
30:29.2	Straight and level	2.6
30:32.8	Left turn	.3
30:37.1	Cruise/decrease thrust	4.9
30:42.2	Cruise/decrease thrust	13.5
30:57.4	Arm command chute	1.6
30:59.2	Command chute	4.0
31:16.0	Arm emergency chute	2.2
31:23.8	Time share (sideslip)	.4
31:34.7	Time share (impact pressure)	.5
31:36.0	Time share (EGT)	.5
31:36.7	Time share (oil pressure)	.7
31:39.2	Strain gage calibrate	3.2
31:44.2	Emergency chute	2.3

TABLE V.- FLIGHT-TEST PARAMETERS

Test point	Test maneuver	Flight time, min:sec	Mach number	Altitude		Aircraft weight		Vertical load factor, g	Dynamic pressure		Angle of attack, deg
				km	ft	N	lbf		kN/m^2	lbf/ft^2	
1	Pull-up	1:05	0.92	[a]0.44	[b]1.3 × 10^3	9821	2208	1.85	57.4	1200	2.40
2	Cruise	2:55	.80	[a].55	[b]1.7	9334	2166	.90	42.9	895	1.85
3	Cruise	4:55	.85	[a]1.35	[b]4.1	9412	2116	.90	44.4	925	1.80
4	Right turn	5:40	.85	[a]1.40	[b]4.3	9327	2097	3.05	44.0	920	4.80
5	Cruise	8:15	.90	2.30	7.0	9056	2036	.95	45.7	955	1.70
6	Cruise	10:35	.94	5.00	15.2	8829	1985	1.00	36.2	755	1.70
7	Left turn	12:30	.86	5.05	15.4	8660	1947	2.95	29.6	620	6.00
8	Climb	14:30	.86	7.95	24.2	8478	1906	.85	21.5	450	2.80
9	Pull-up	16:45	1.07	10.60	32.3	8020	1803	1.70	23.1	480	2.95
10	Cruise	17:45	1.06	10.95	33.4	7966	1791	.95	21.2	445	1.35
11	Left turn	19:30	1.08	11.75	35.8	7864	1768	2.00	19.7	410	4.10
12	Cruise	21:40	1.13	11.75	35.8	7731	1738	.95	20.3	425	1.60
13	Dive	23:50	1.18	7.20	21.9	7642	1718	.85	42.5	890	.50
14	Pull-up	24:05	1.13	4.80	14.6	7624	1714	2.25	52.6	1100	1.50
15	Pull-up	25:52	.94	2.25	6.9	7522	1691	2.00	51.1	1070	1.60
16	Pull-up	27:28	.96	2.20	6.7	7401	1664	2.00	52.7	1100	1.45
17	Pull-up	28:53	.93	2.75	8.4	7925	1640	1.85	44.9	935	1.55
18	Right turn	30:20	.88	4.45	13.6	7152	1608	5.10	33.3	695	6.35
Estimated accuracies			±0.04	±0.20	±0.6 × 10^3	±50	±10	±0.20	±1.2	±25	±0.20

[a]Estimated accuracy ±0.06.

[b]Estimated accuracy ±0.2 × 10^3.

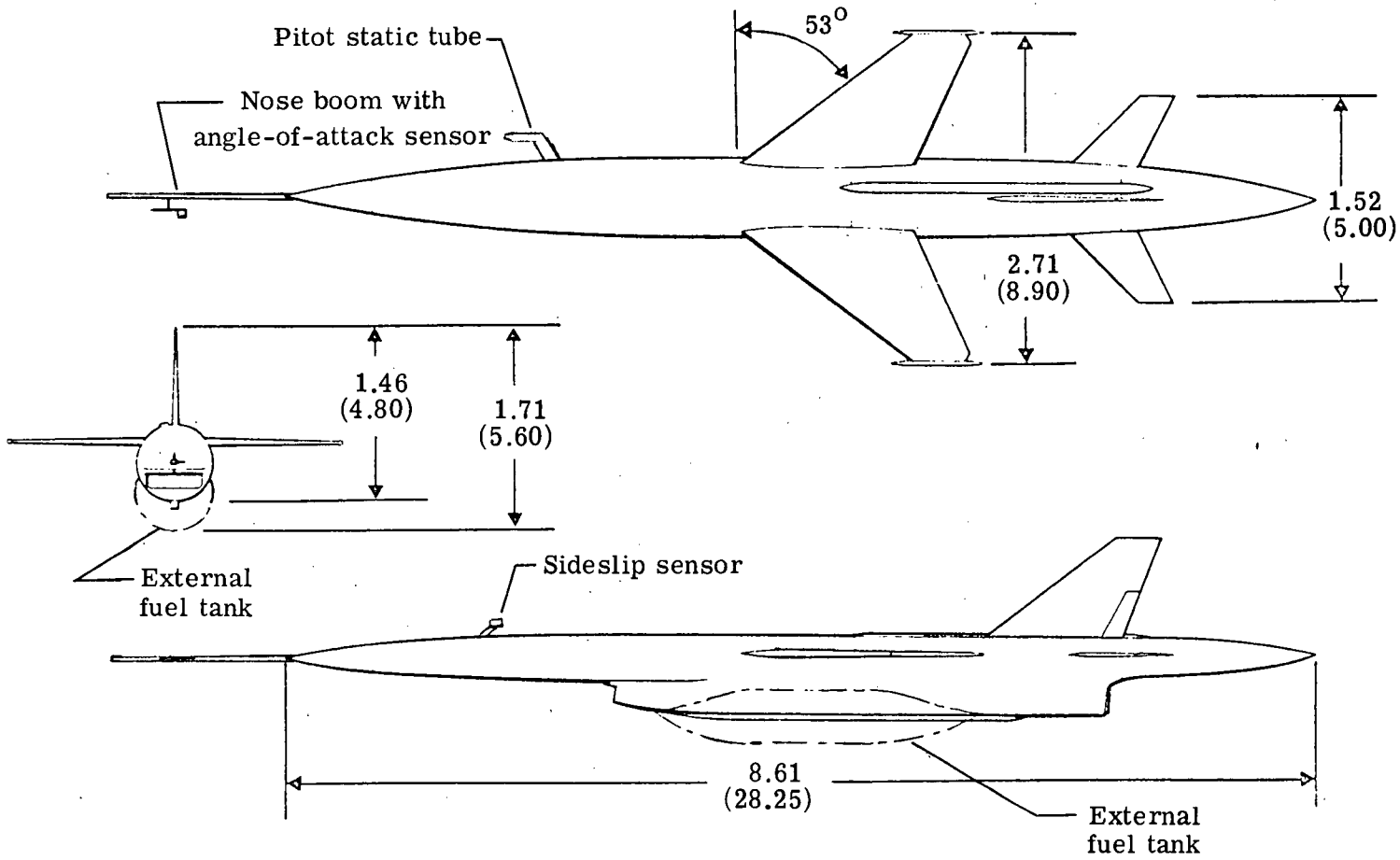

Figure 1.- Three views of test vehicle. (Dimensions are in meters (ft).)

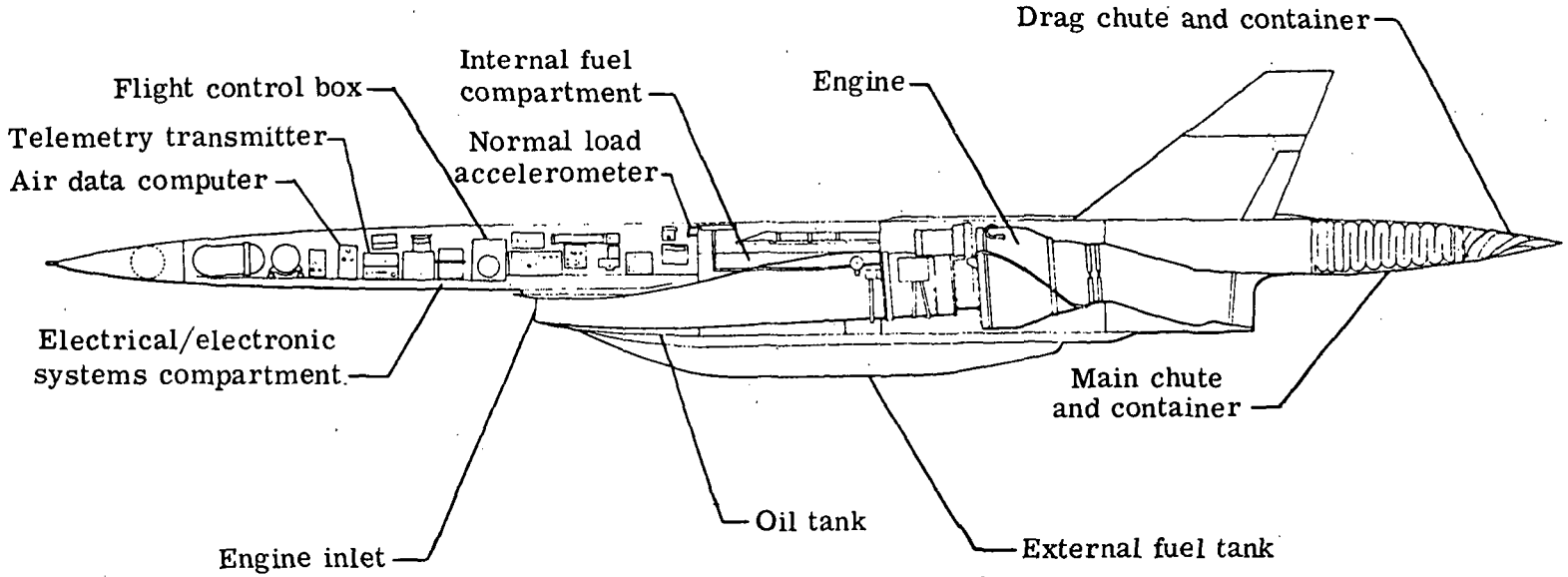

Figure 2.- Inboard profile of test vehicle.

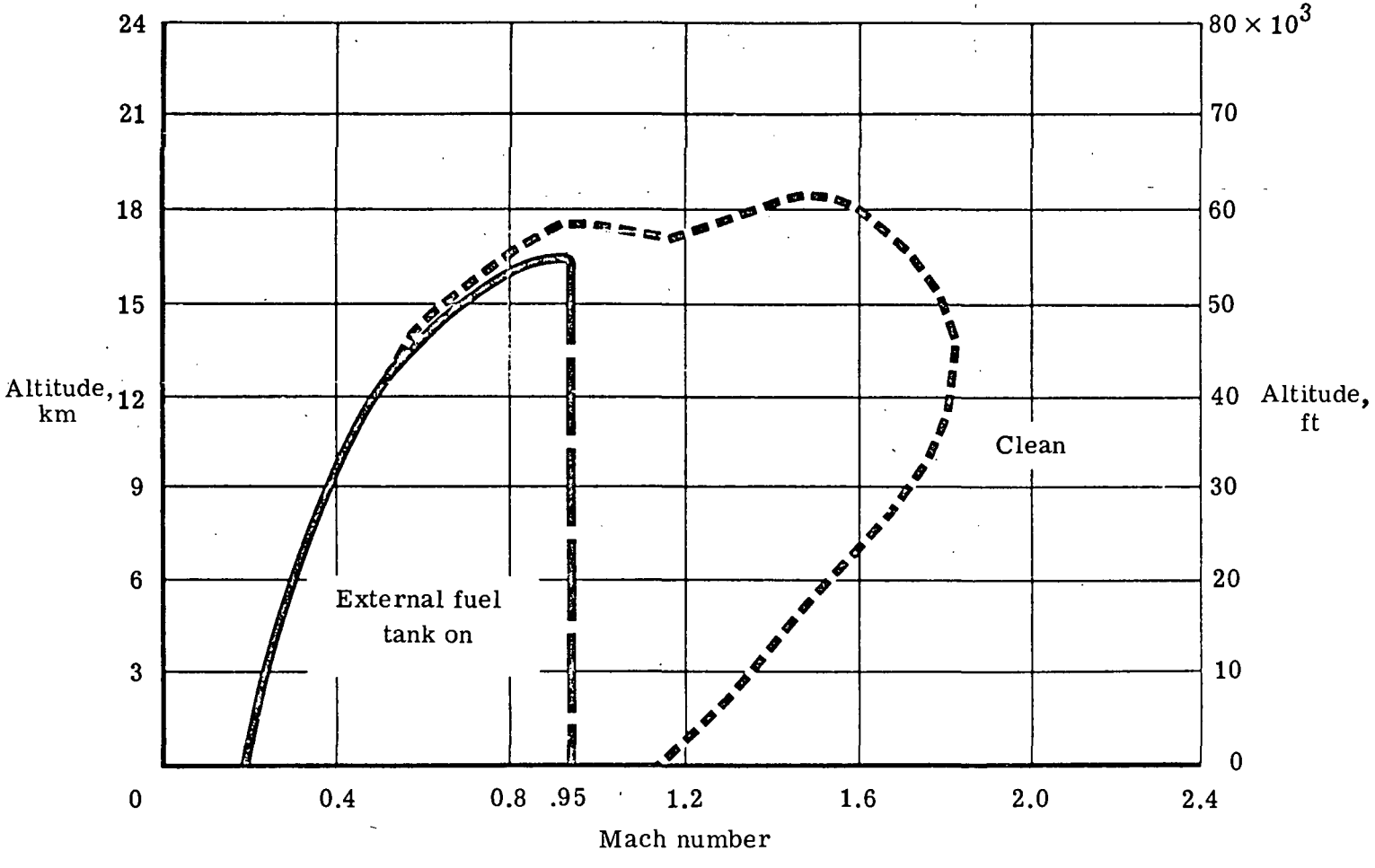

Figure 3.- Standard vehicle speed-altitude envelope.

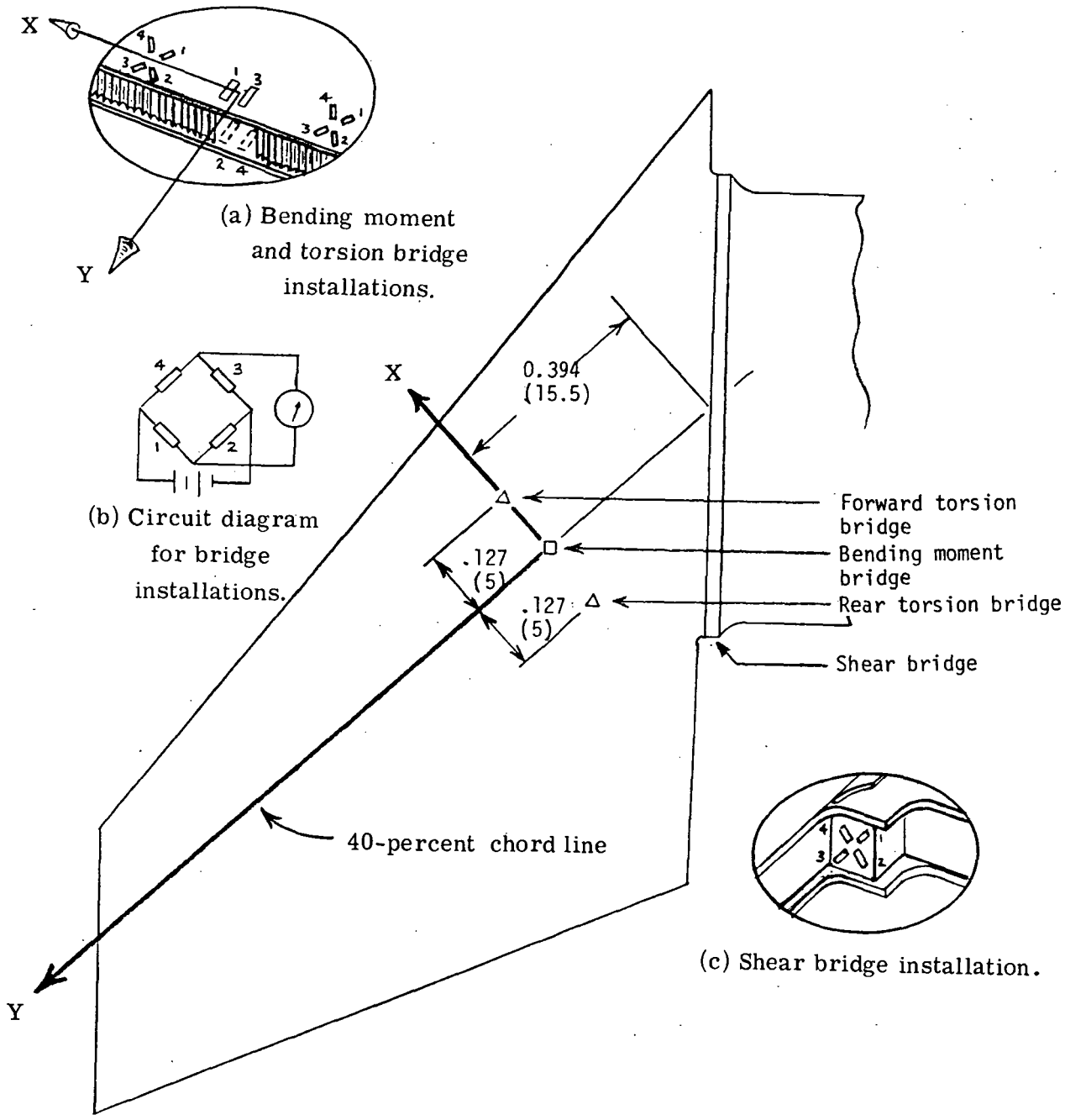

Figure 4.- Location of strain gage bridges. (Dimensions are in meters (in.).)

Not used for research flight

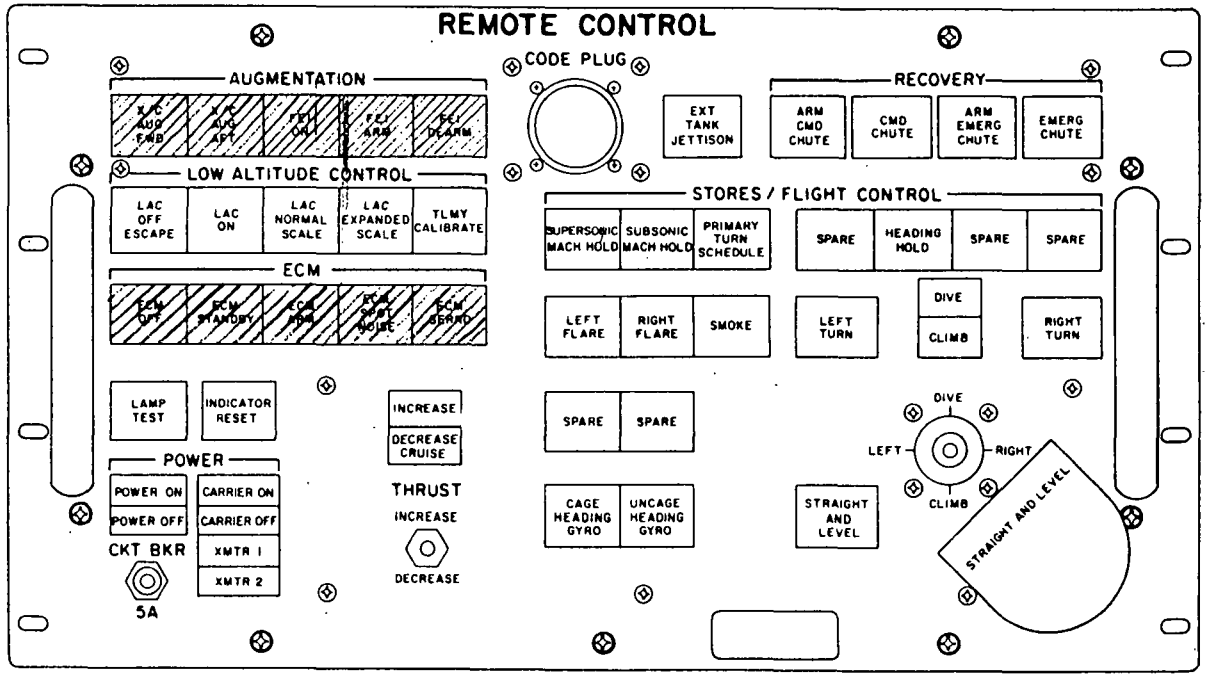

Figure 5.- Layout of remote control panel.

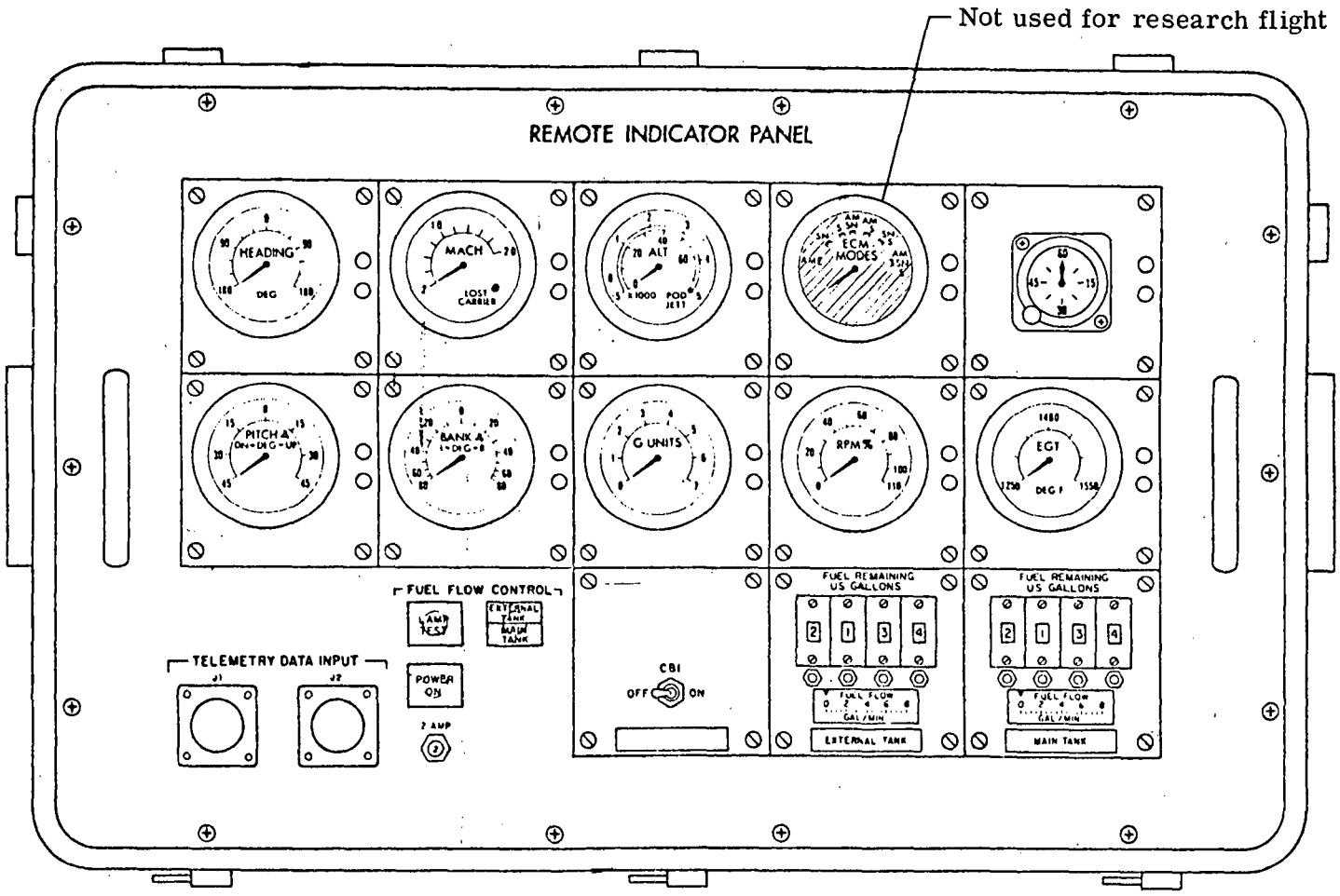

Figure 6.- Remote indicator panel.

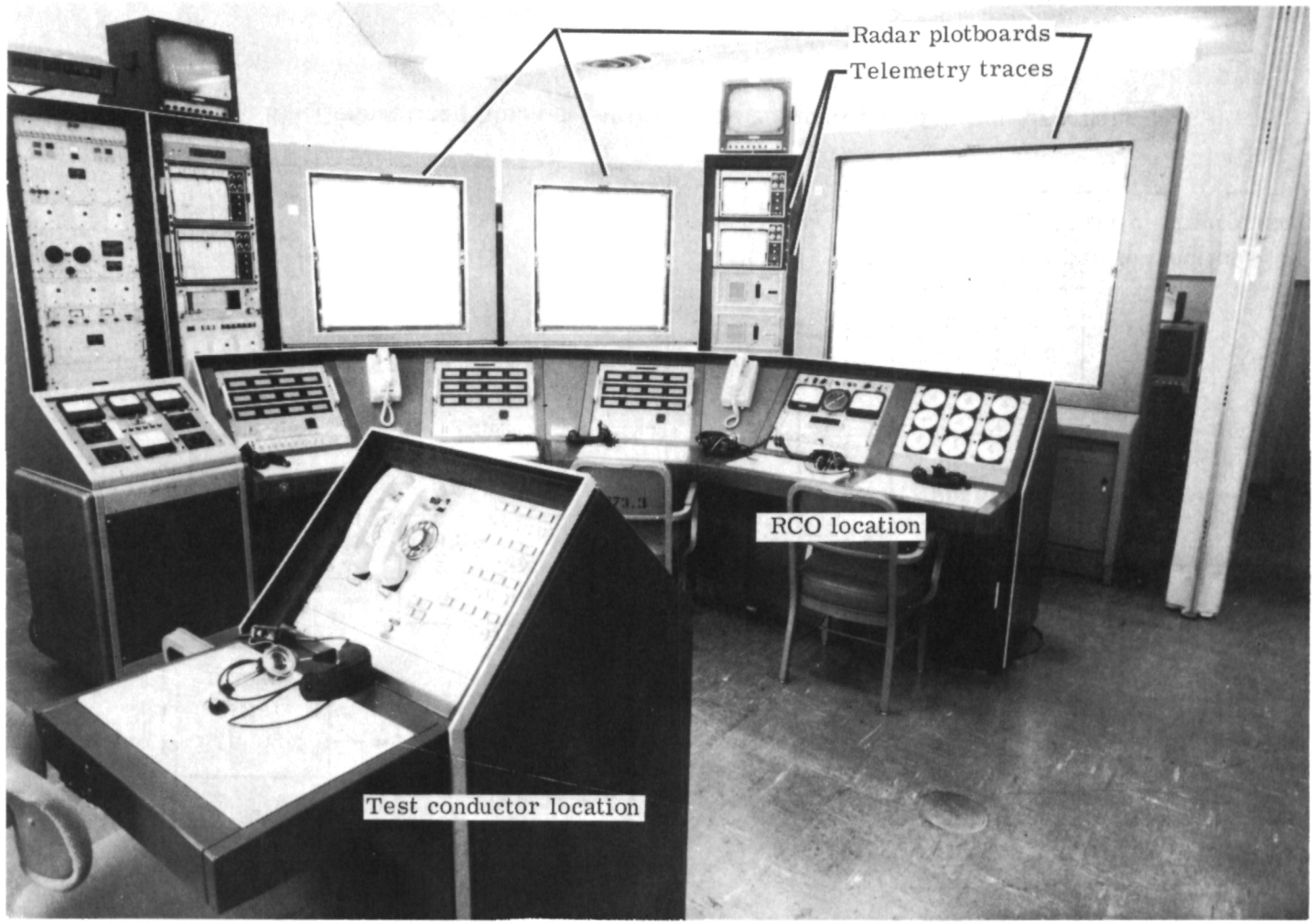

Figure 7.- Photograph of a typical control center. U.S. Navy photograph.

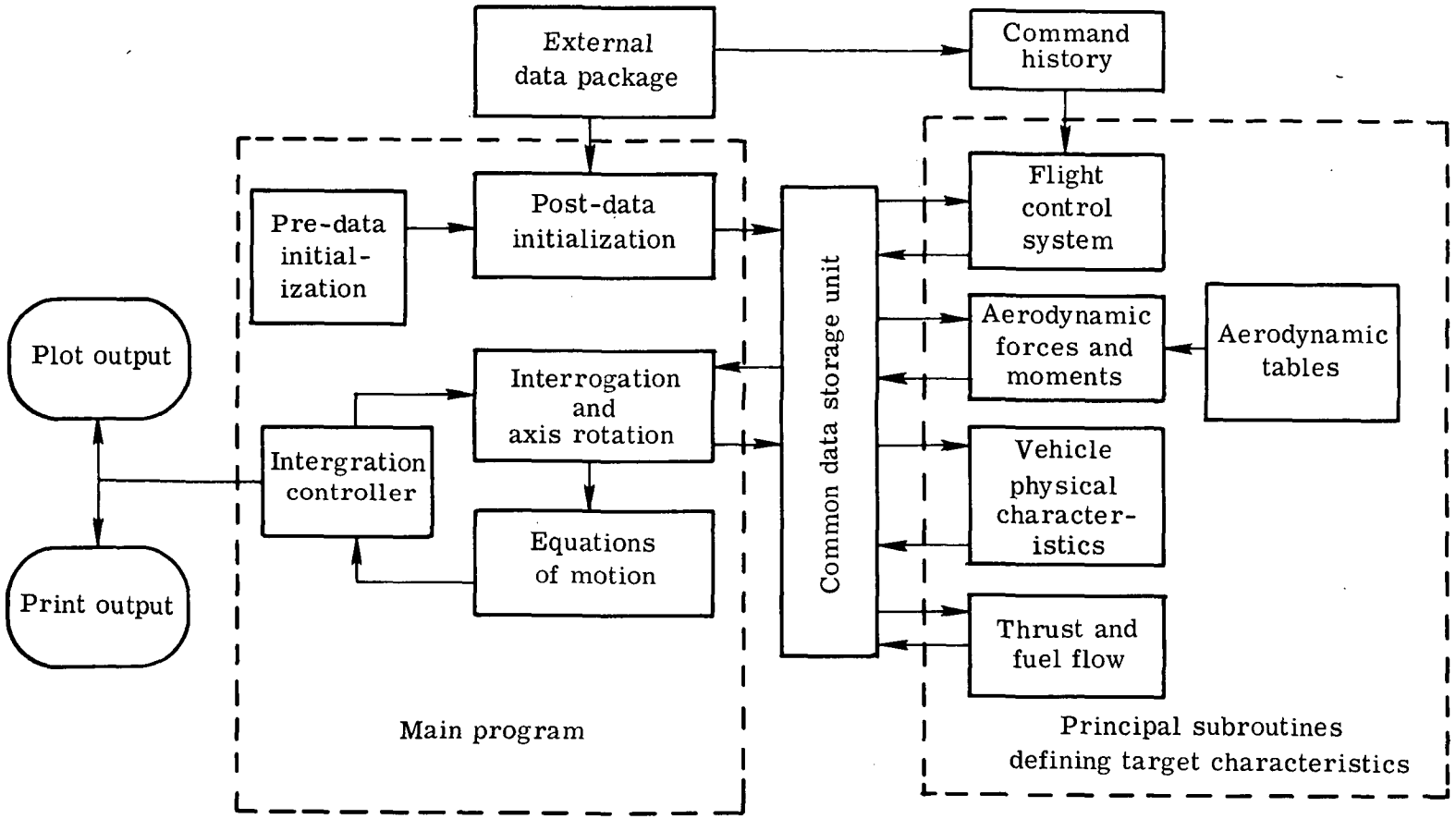

Figure 8.- Generalized block diagram of the computer simulation program.

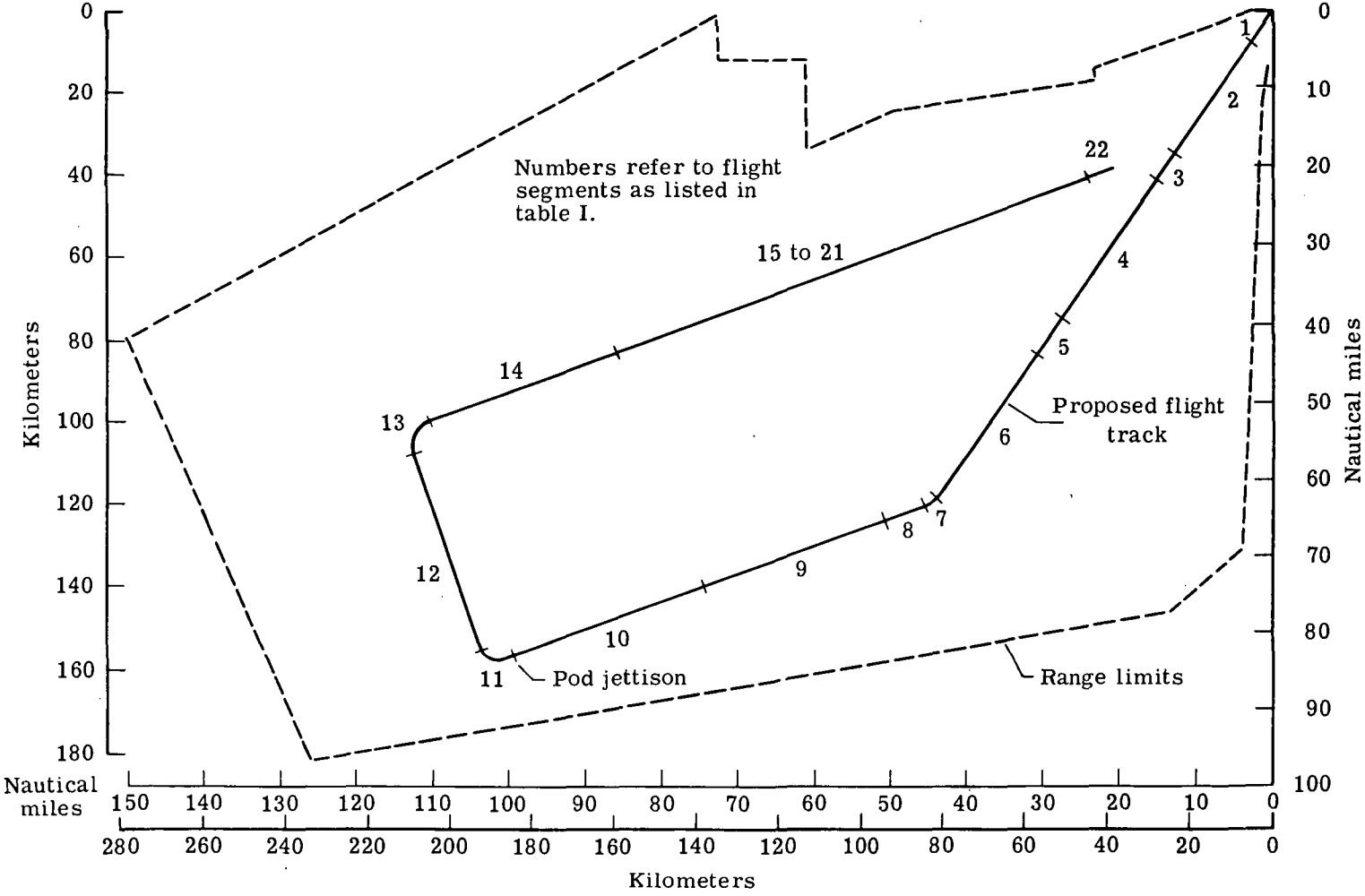

Figure 9.- Plan view of initial flight plan.

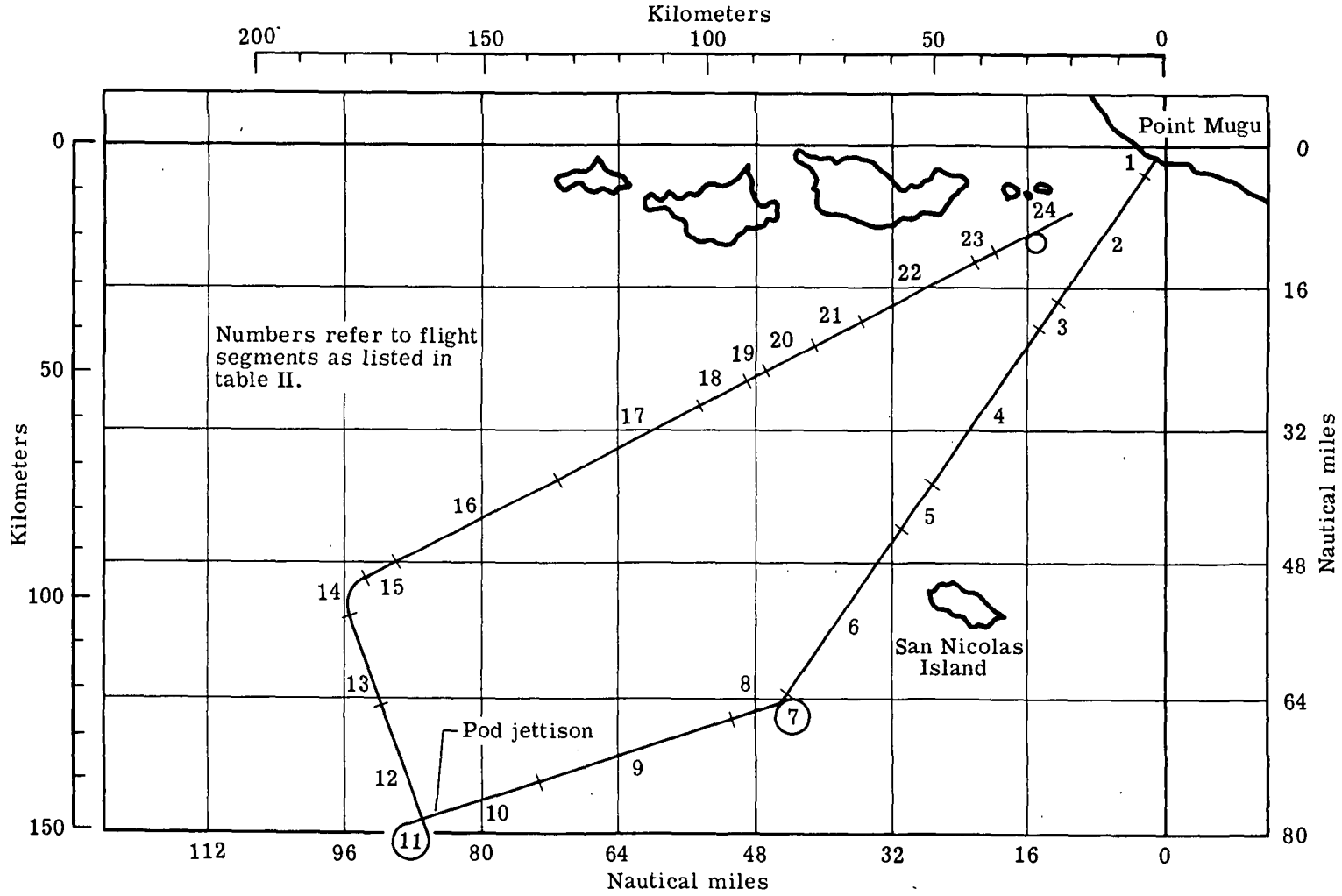

Figure 10.- Plan view of flight for ground launch.

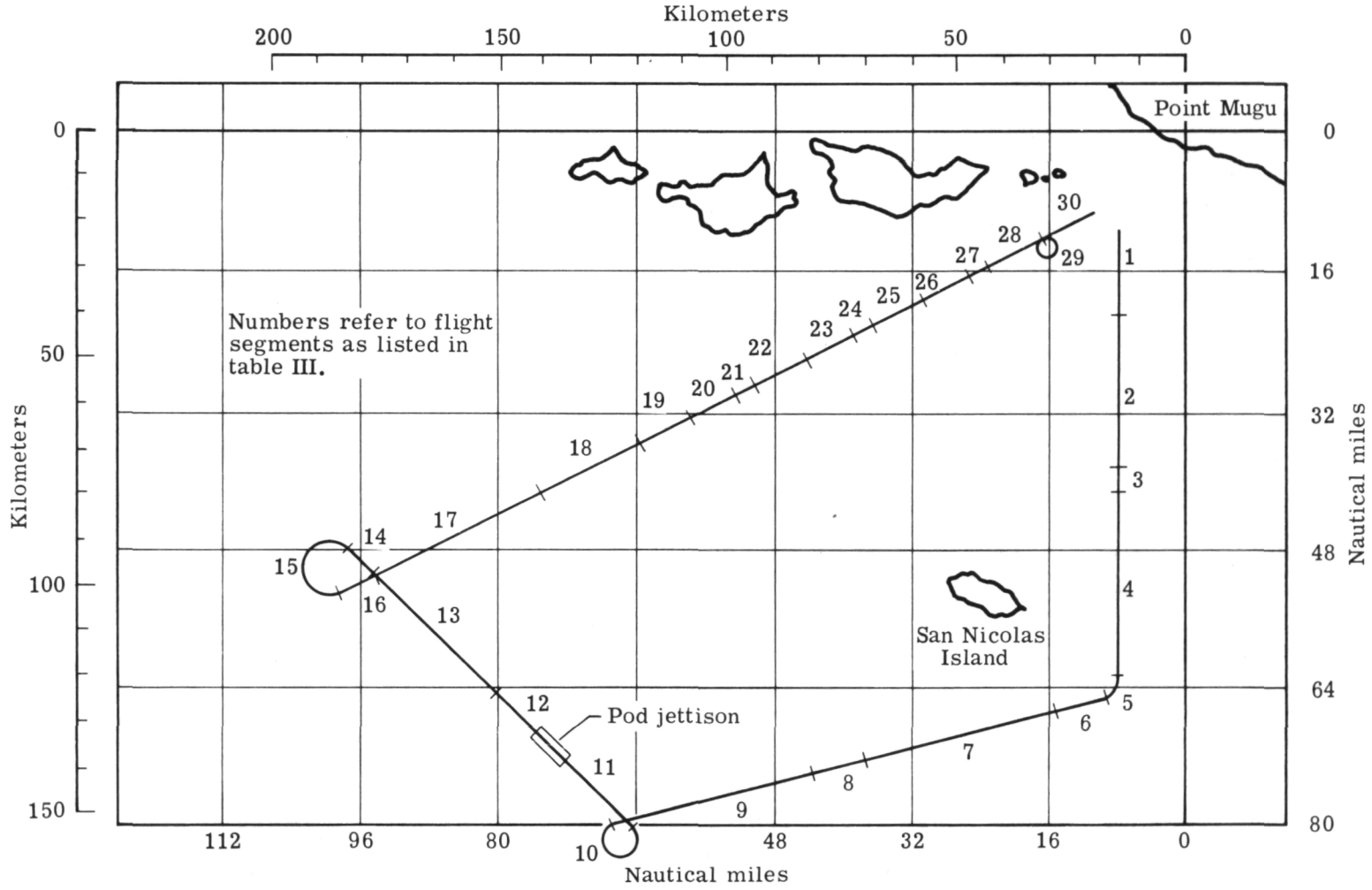

Figure 11.- Plan view of flight for air launch.

Figure 12.- The BQM-34E suspended from the wing of the P-2V launch aircraft. U.S. Navy photograph.

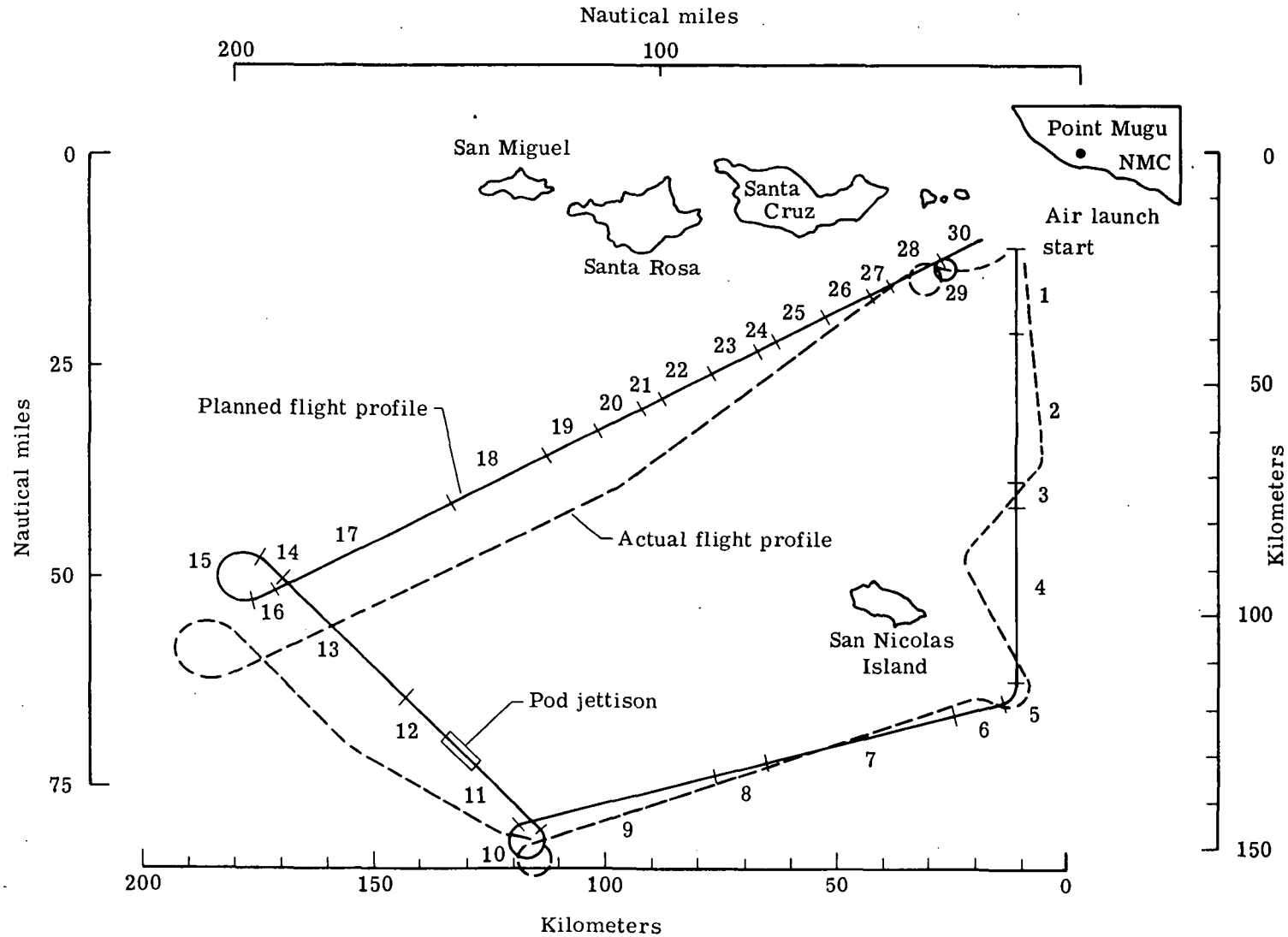

Figure 13.- Actual flight-test flight plan view (radar plotboard).

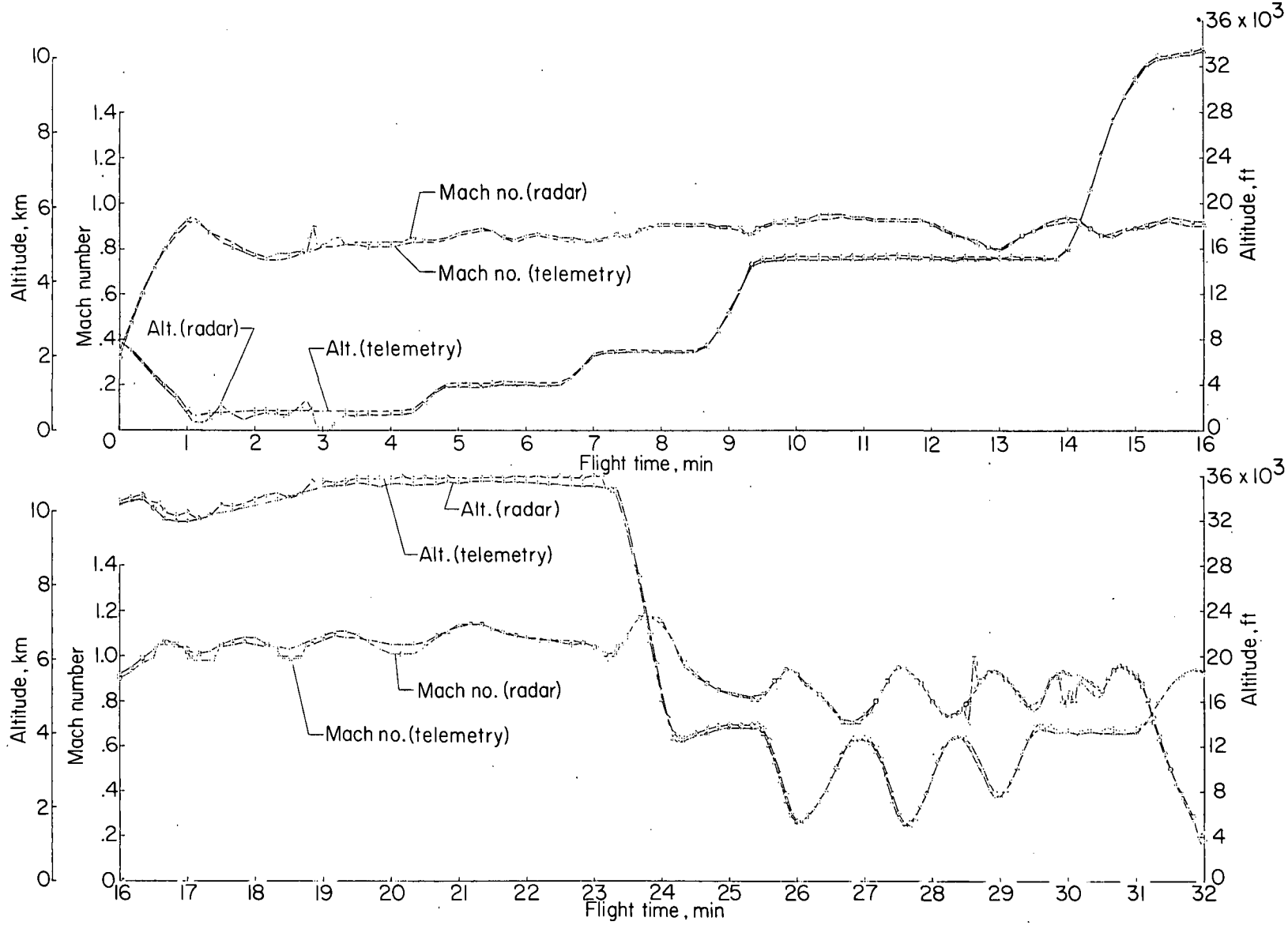

Figure 14.- Flight Mach number and altitude as determined by onboard measurements (telemetry) and by radar tracking.

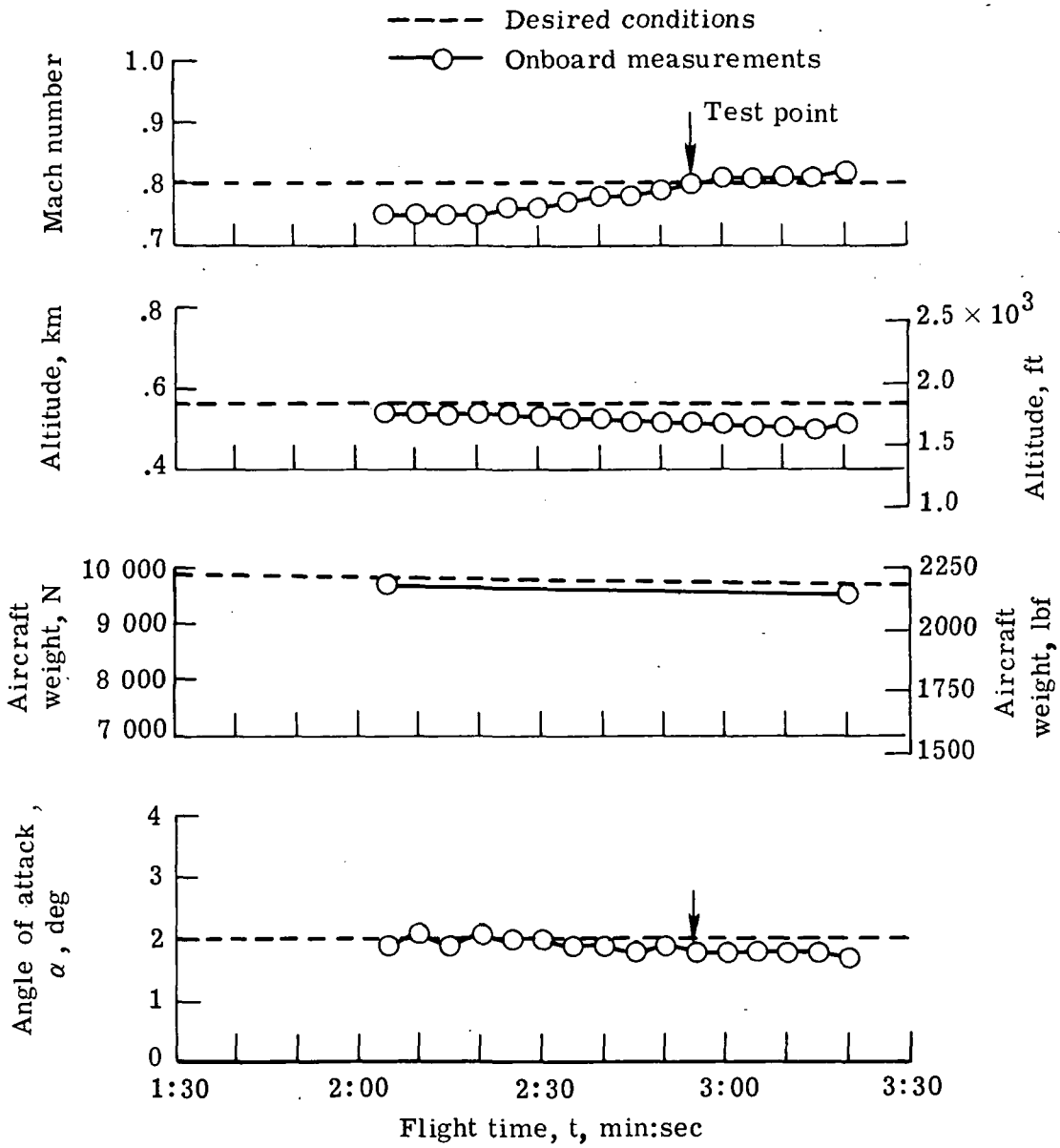

Figure 15.- Flight-test conditions for cruise at M = 0.80.

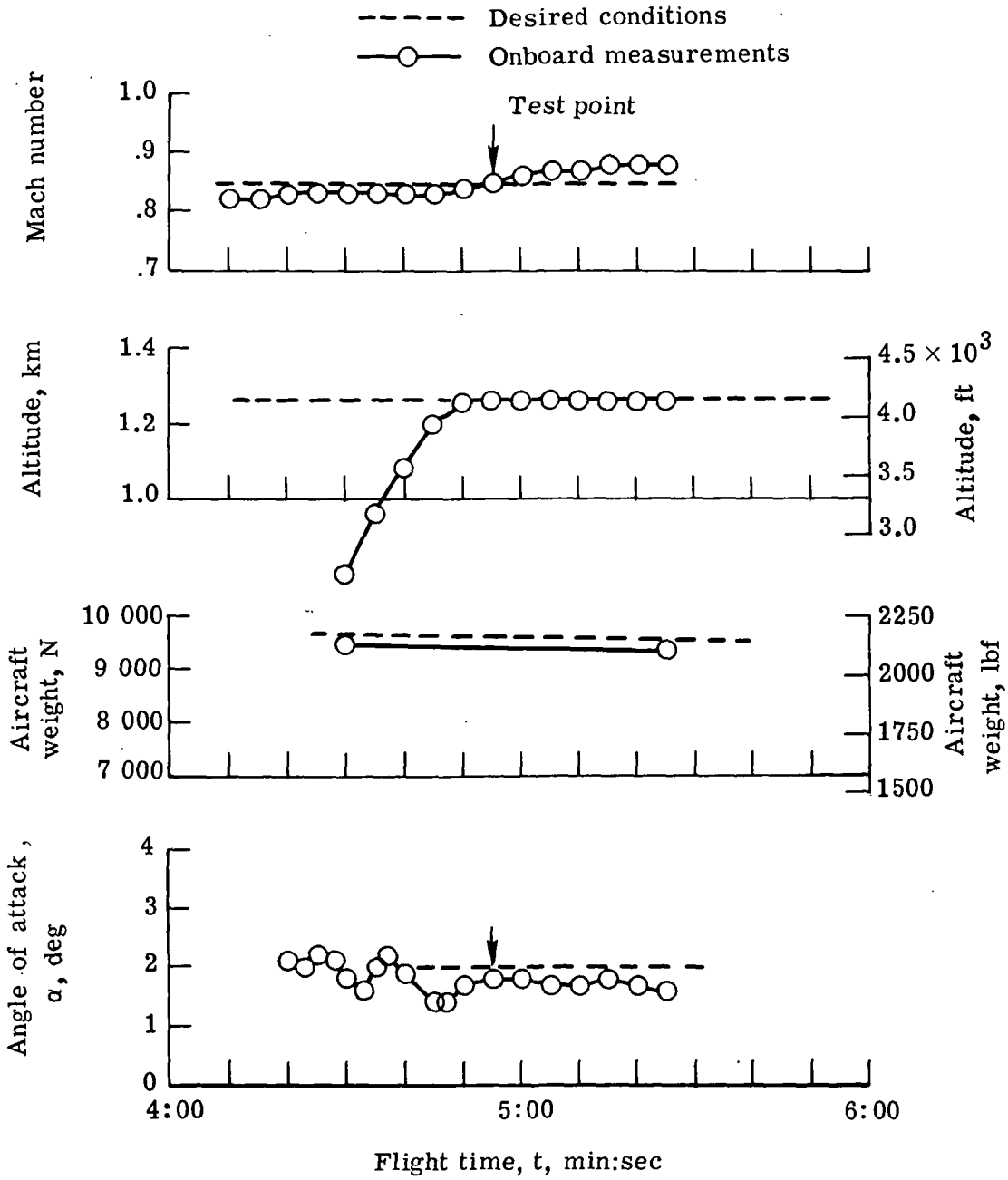

Figure 16.- Flight-test conditions for cruise at M = 0.85.

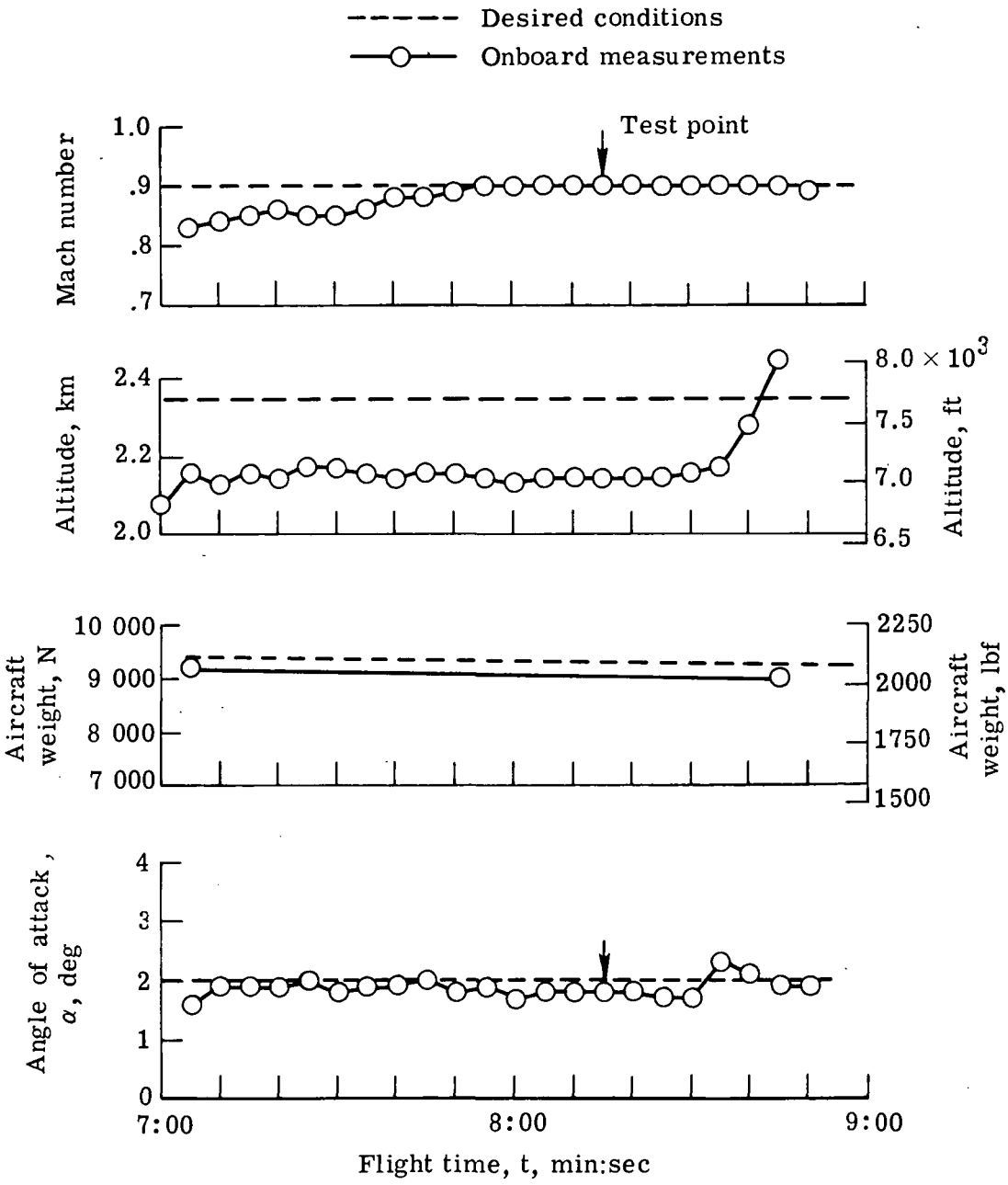

Figure 17.- Flight-test conditions for cruise at M = 0.90.

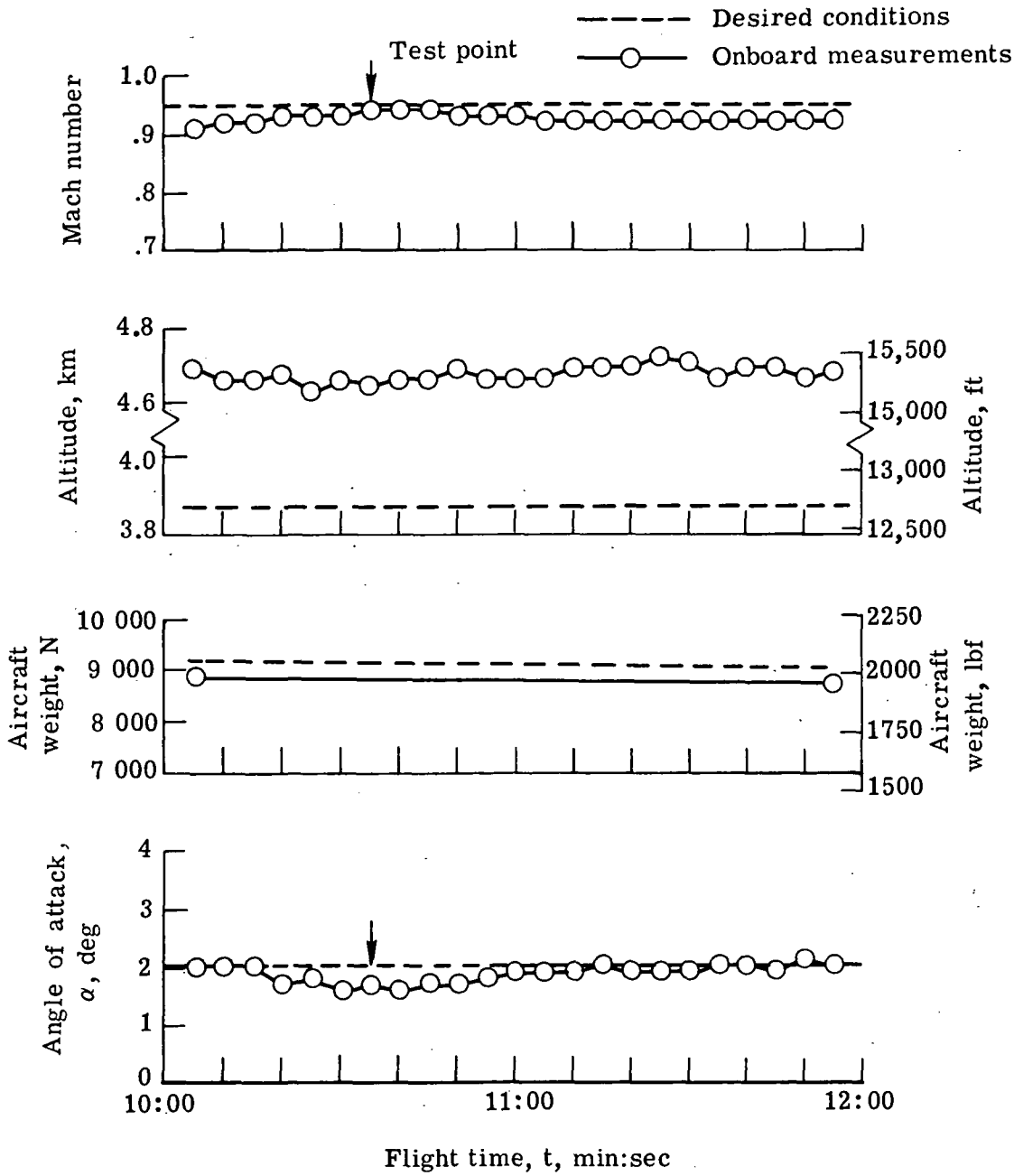

Figure 18.- Flight-test conditions for cruise at M = 0.95.

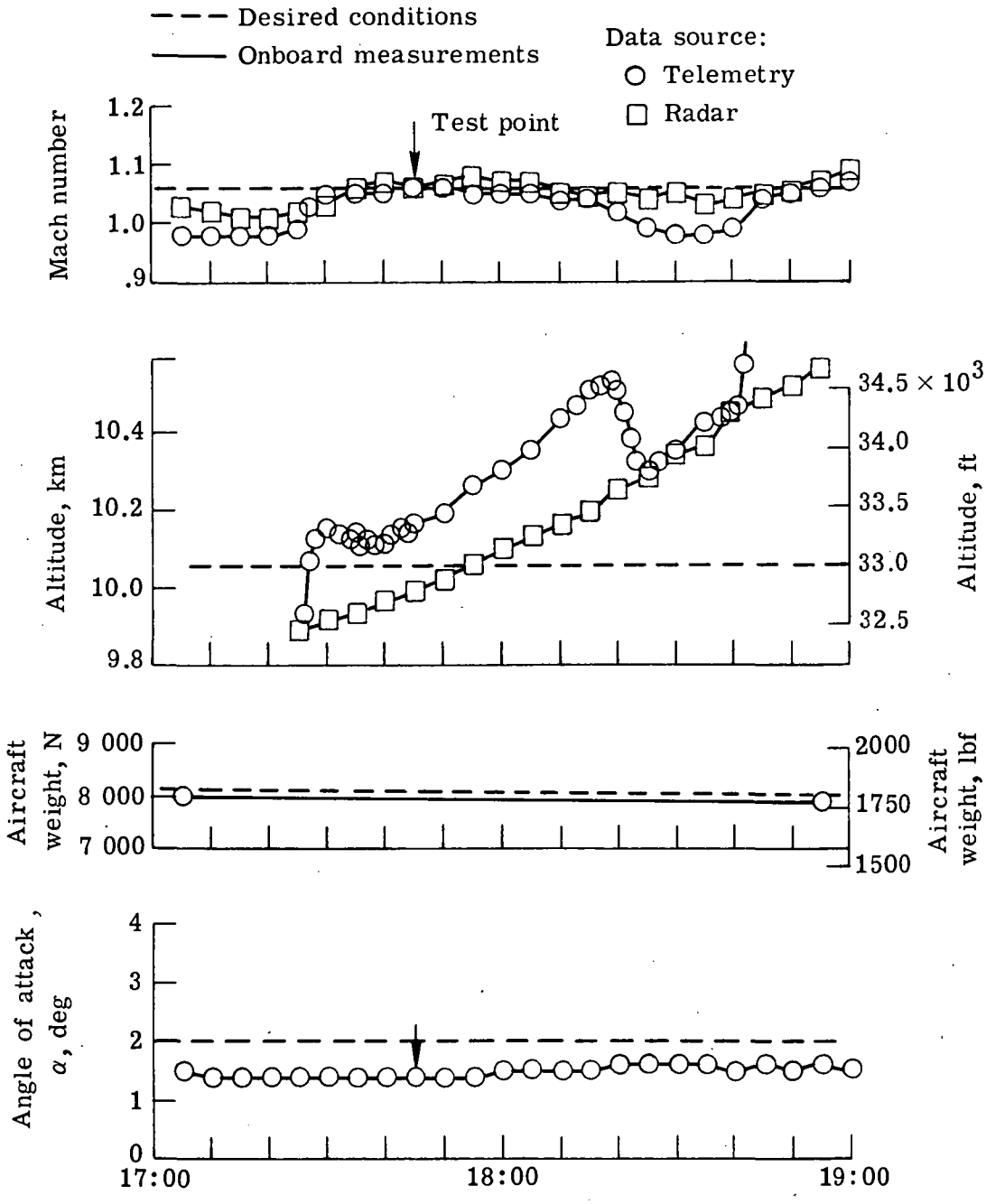

Figure 19.- Flight-test conditions for cruise at M = 1.06.

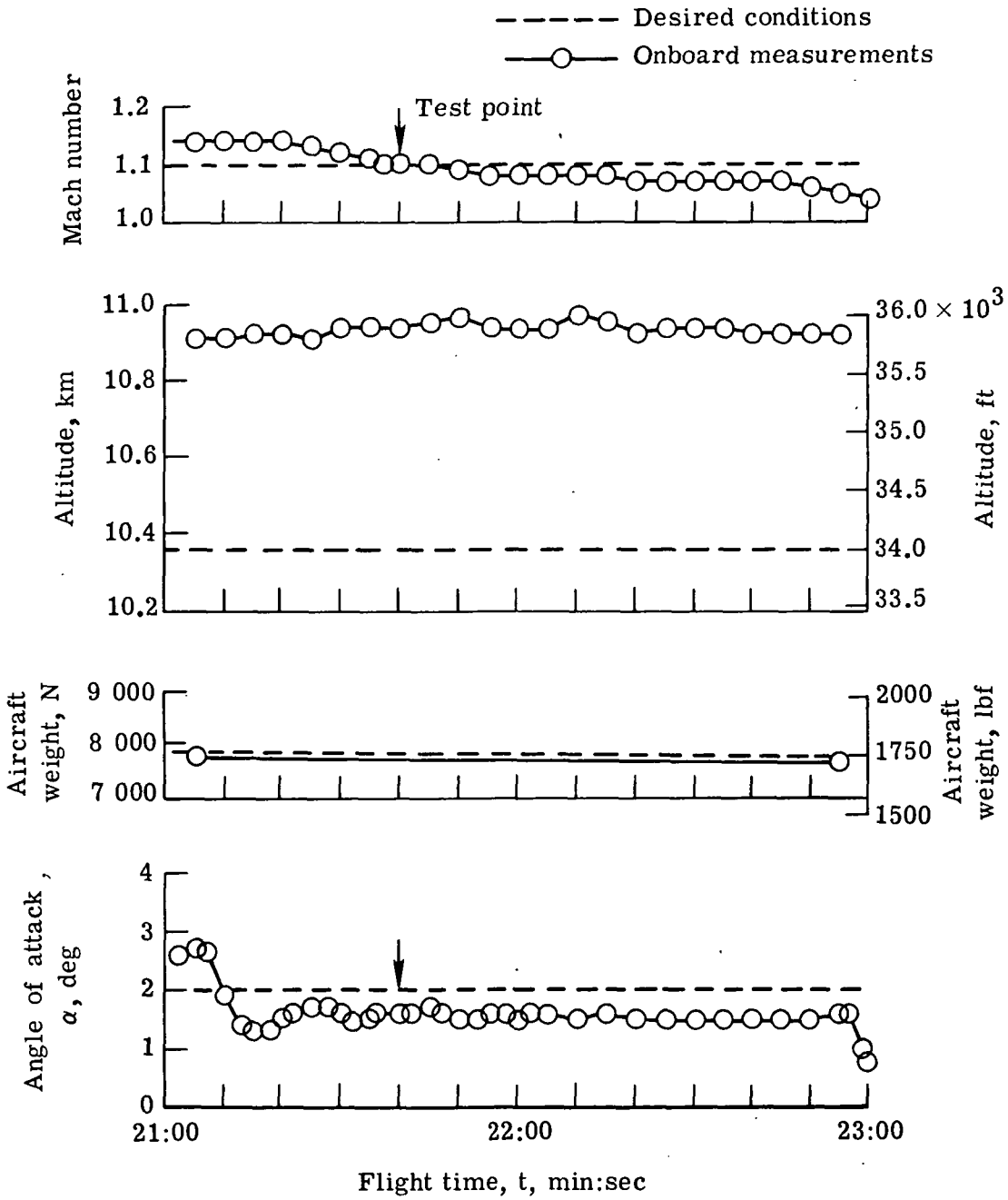

Figure 20.- Flight-test conditions for cruise at M = 1.10.

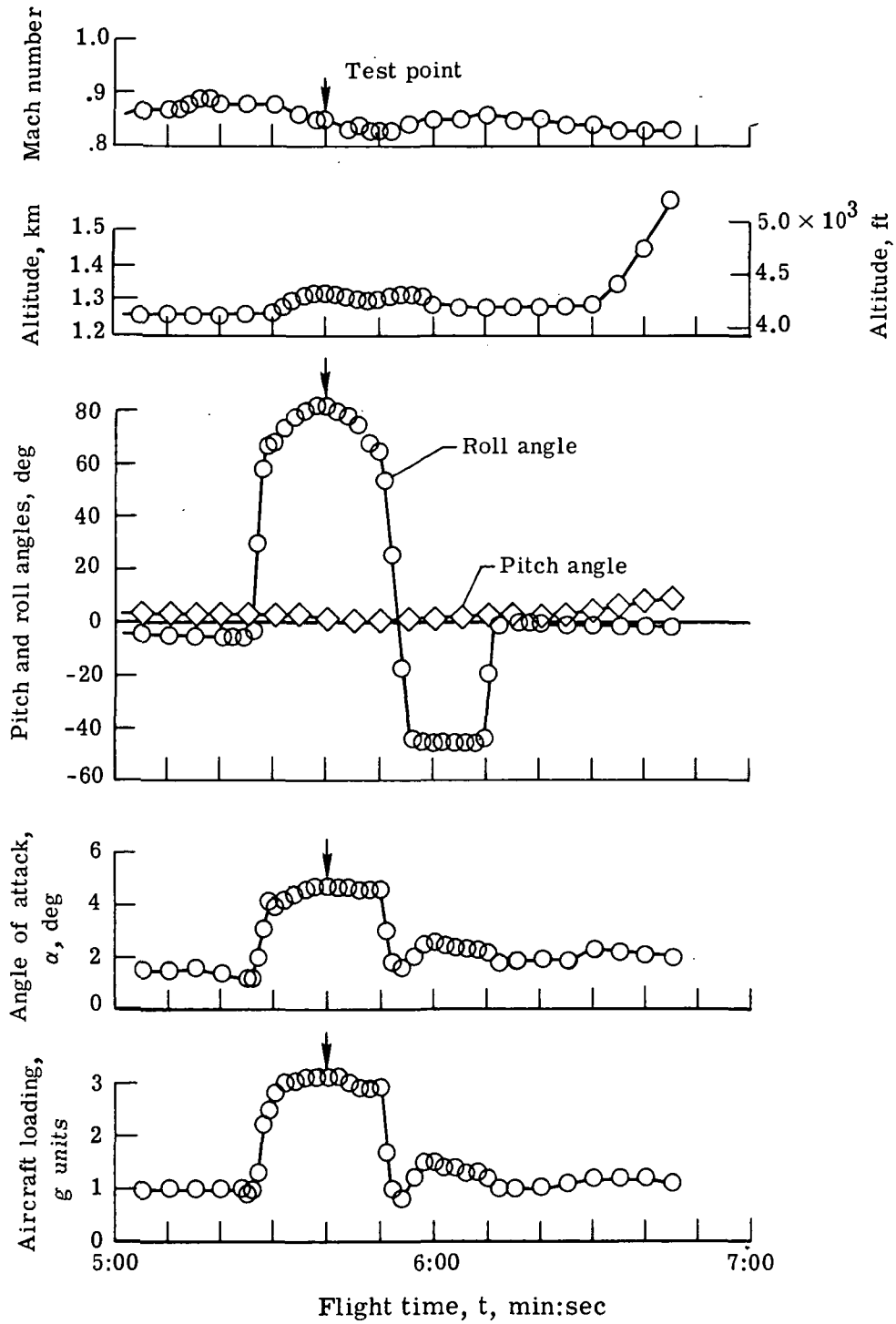

Figure 21.- Flight-test conditions during the first g-controlled turn.

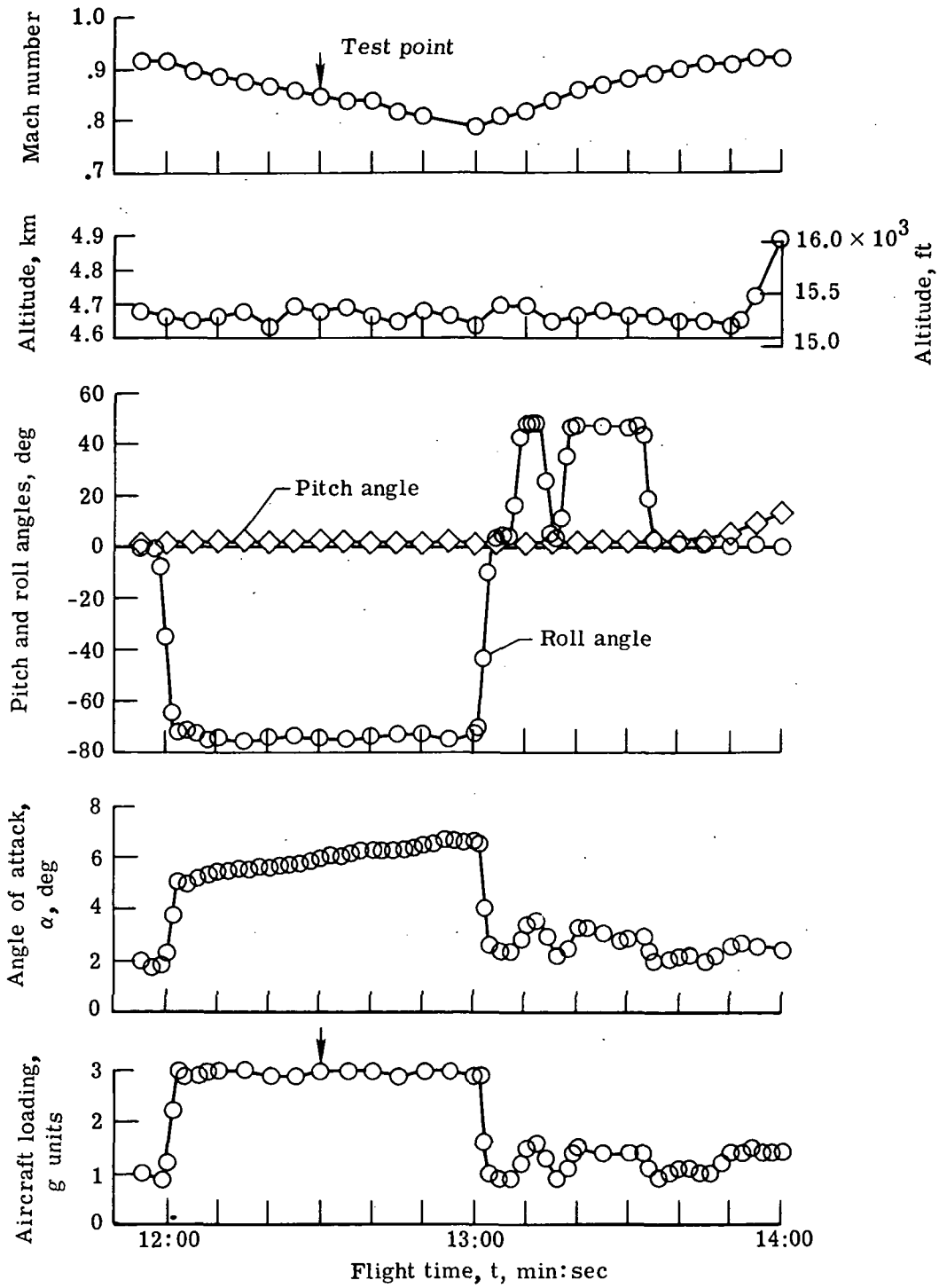

Figure 22.- Flight-test conditions during the second g-controlled turn.

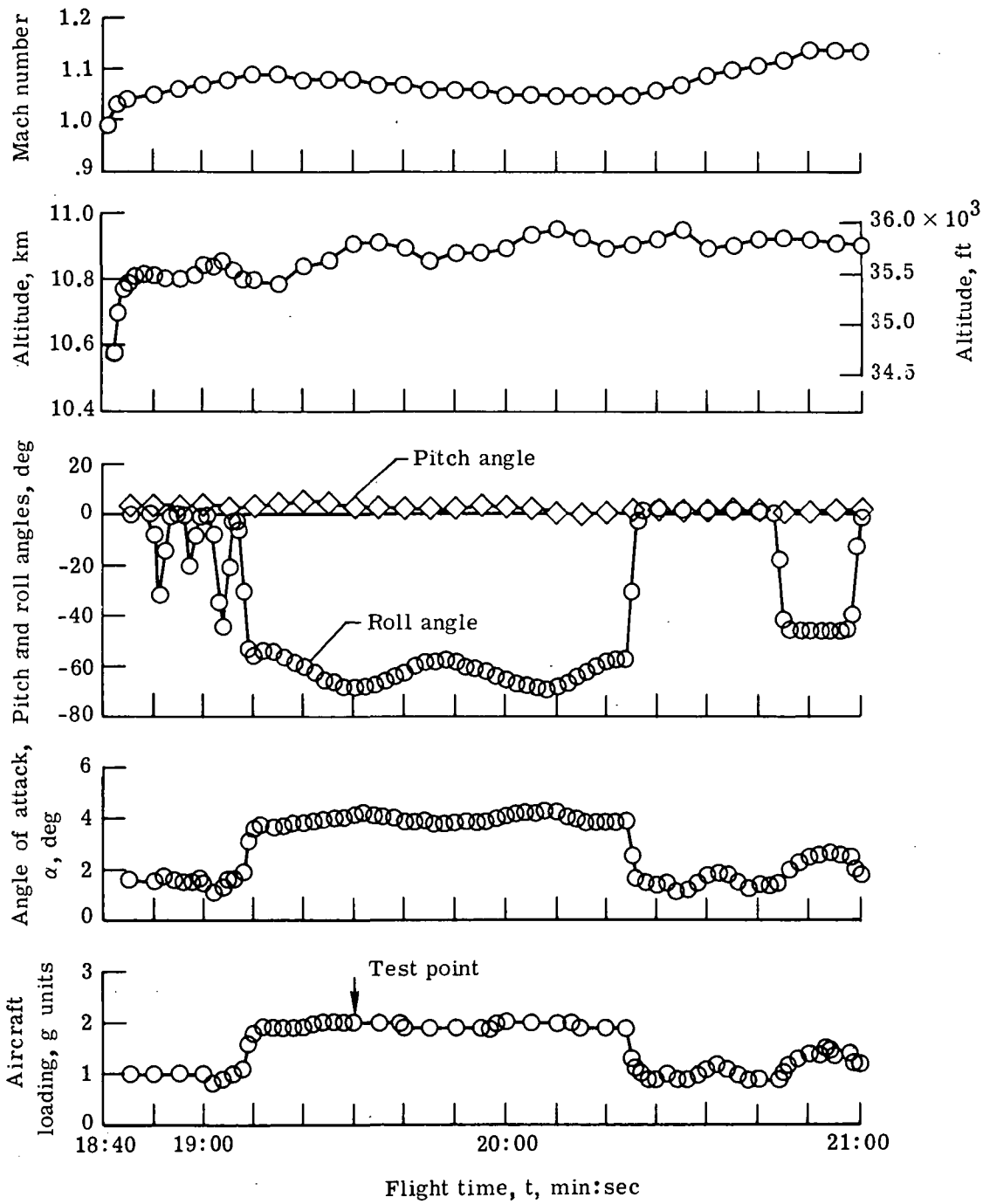

Figure 23.- Flight-test conditions during the third g-controlled turn.

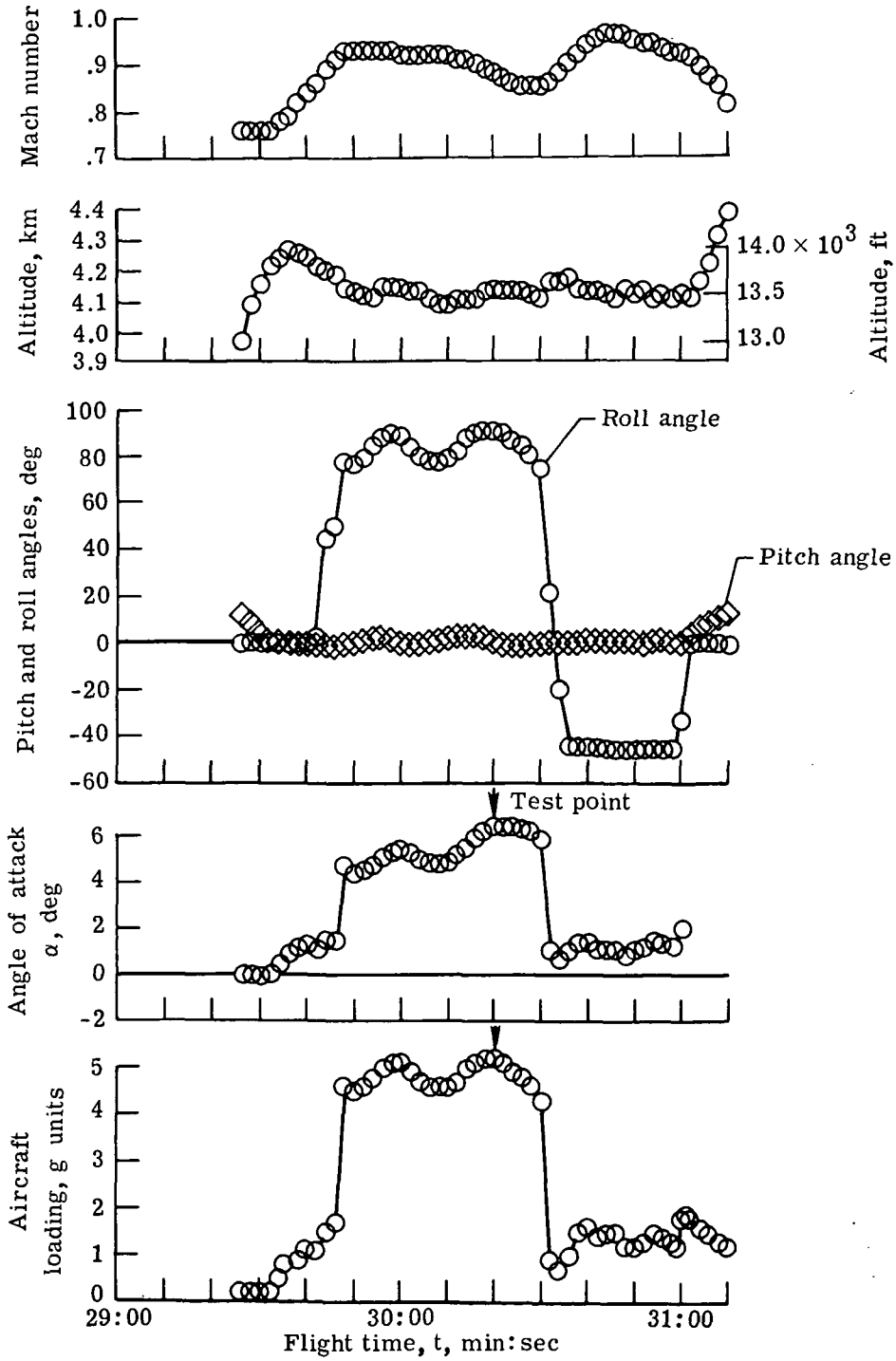

Figure 24.- Flight-test conditions during the fourth g-controlled turn.

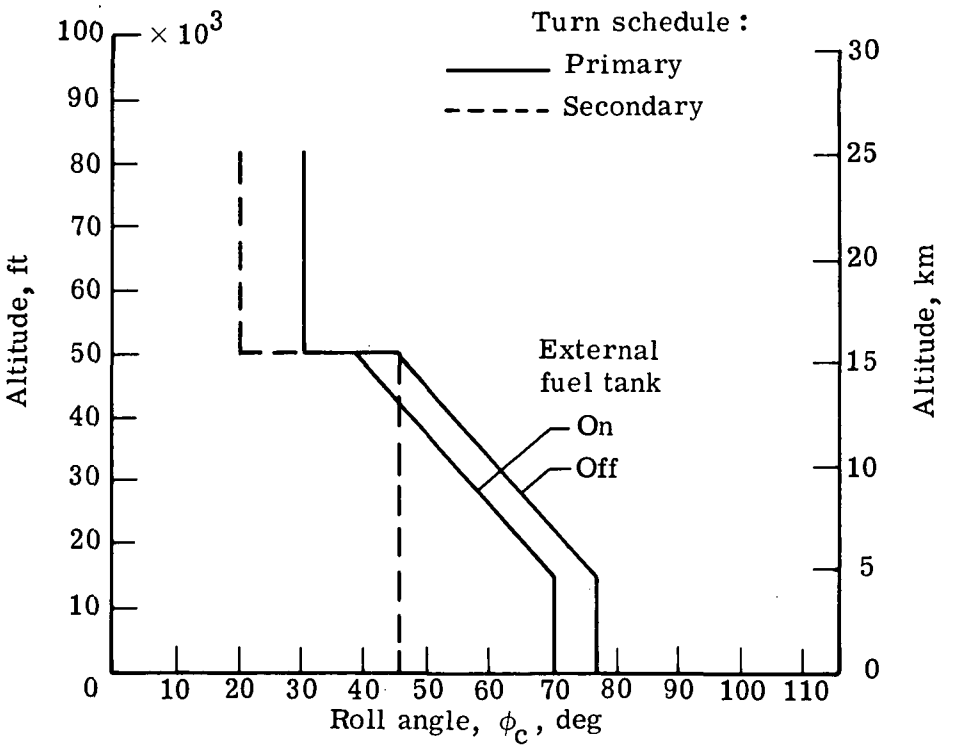

Figure 25.- Turn-schedule roll angles as a function of altitude, command turn schedule, and vehicle configuration.

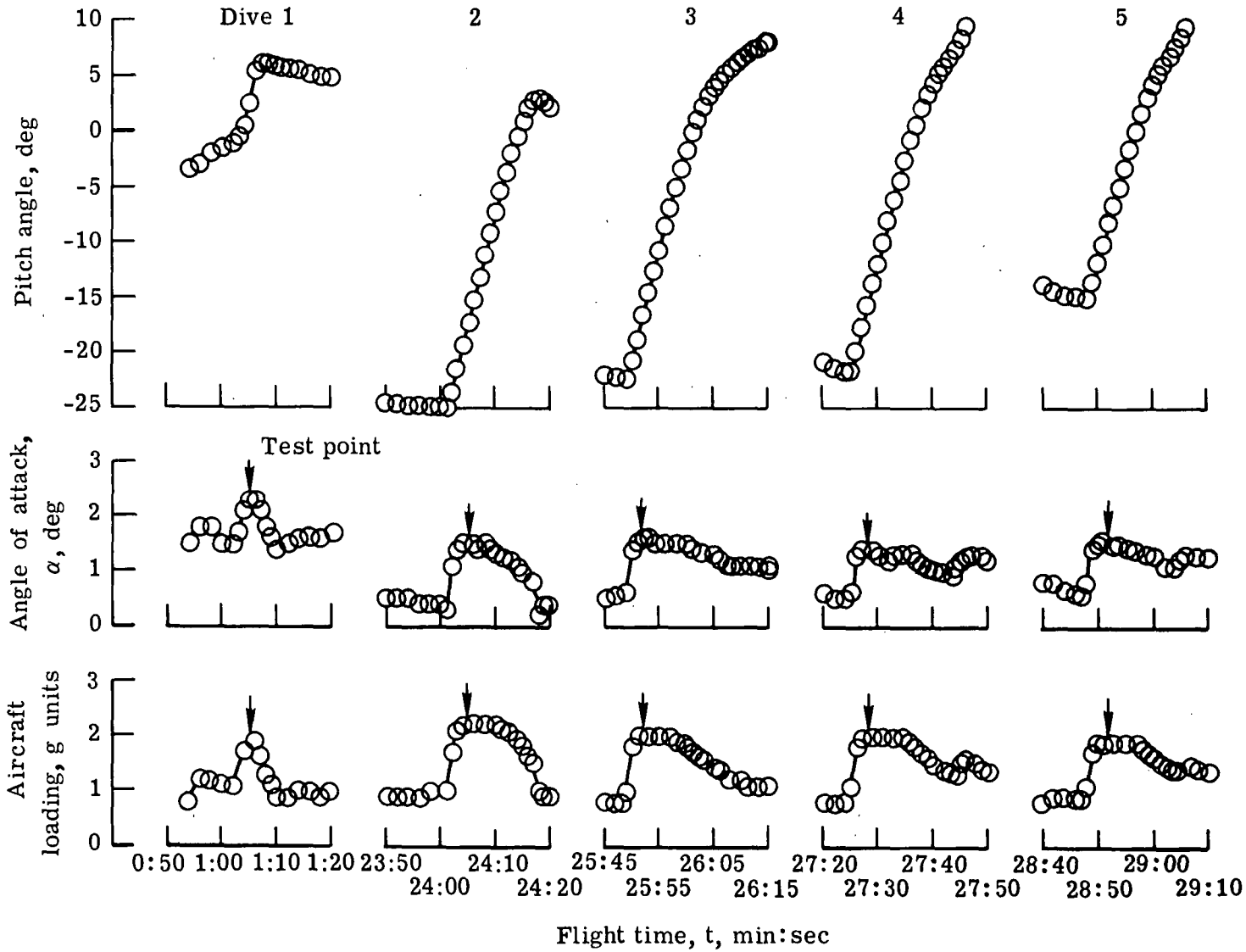

Figure 26.- Flight-test conditions for the five pull-up maneuvers.

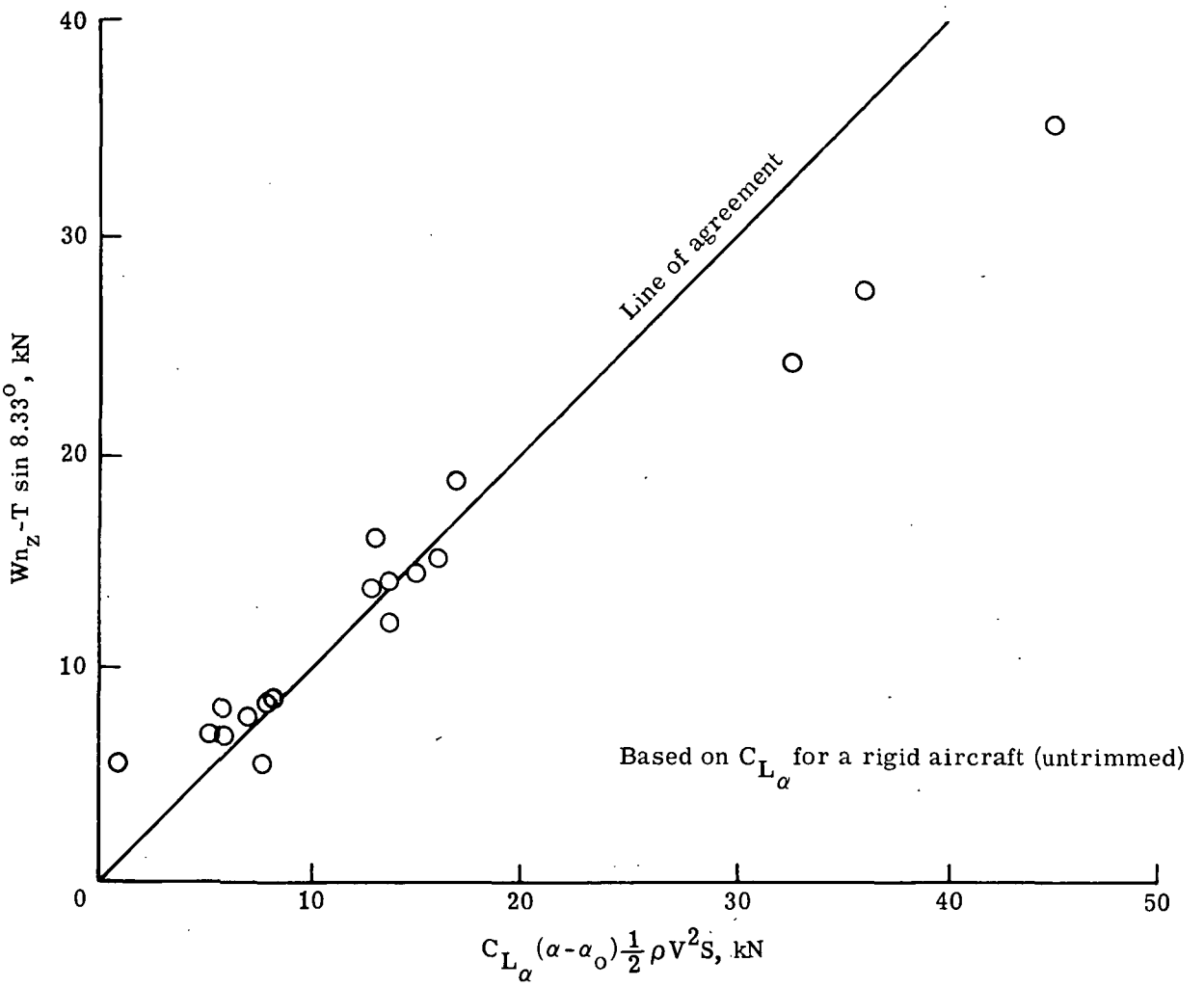

Figure 27.- Comparison of normal forces based on C_{L_α} for a rigid aircraft.

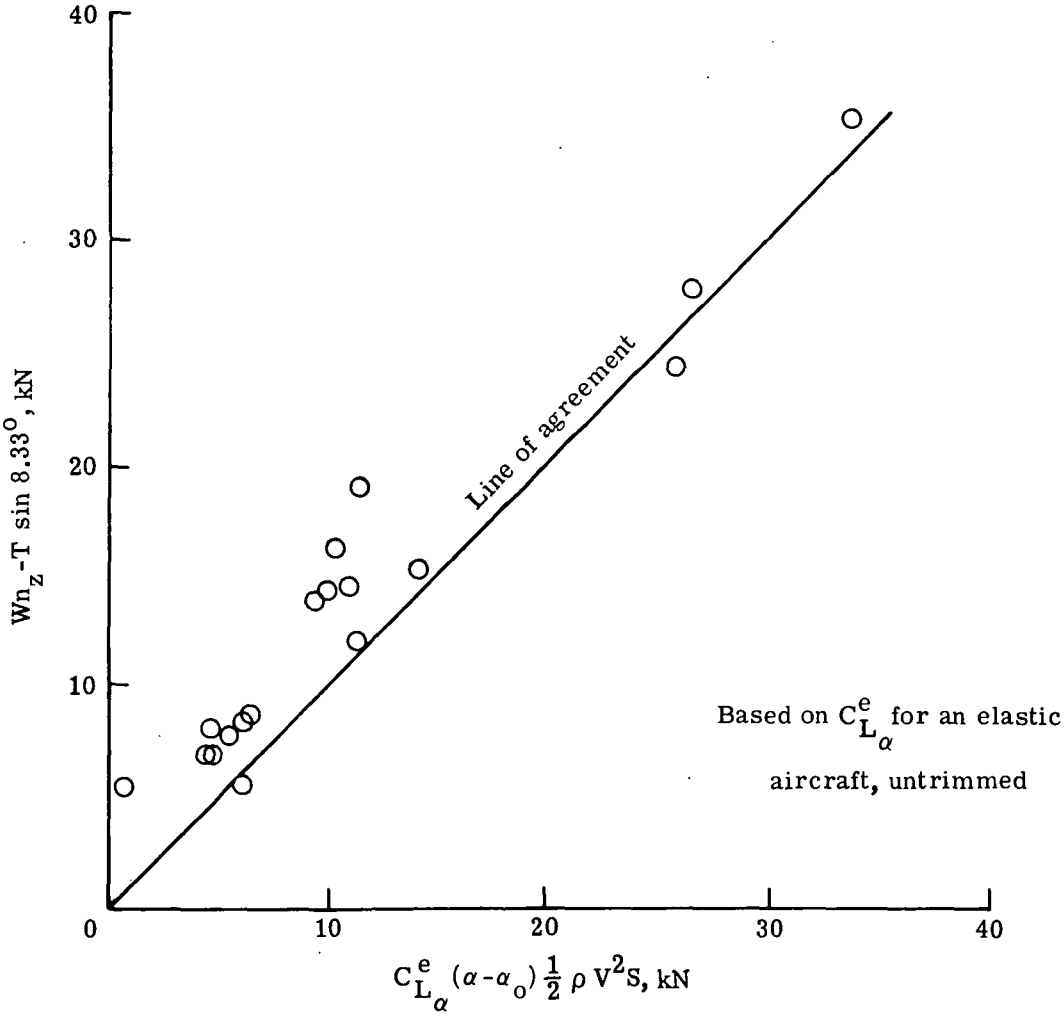

Figure 28.- Comparison of normal forces based on $C^e_{L_\alpha}$ for an untrimmed elastic aircraft.

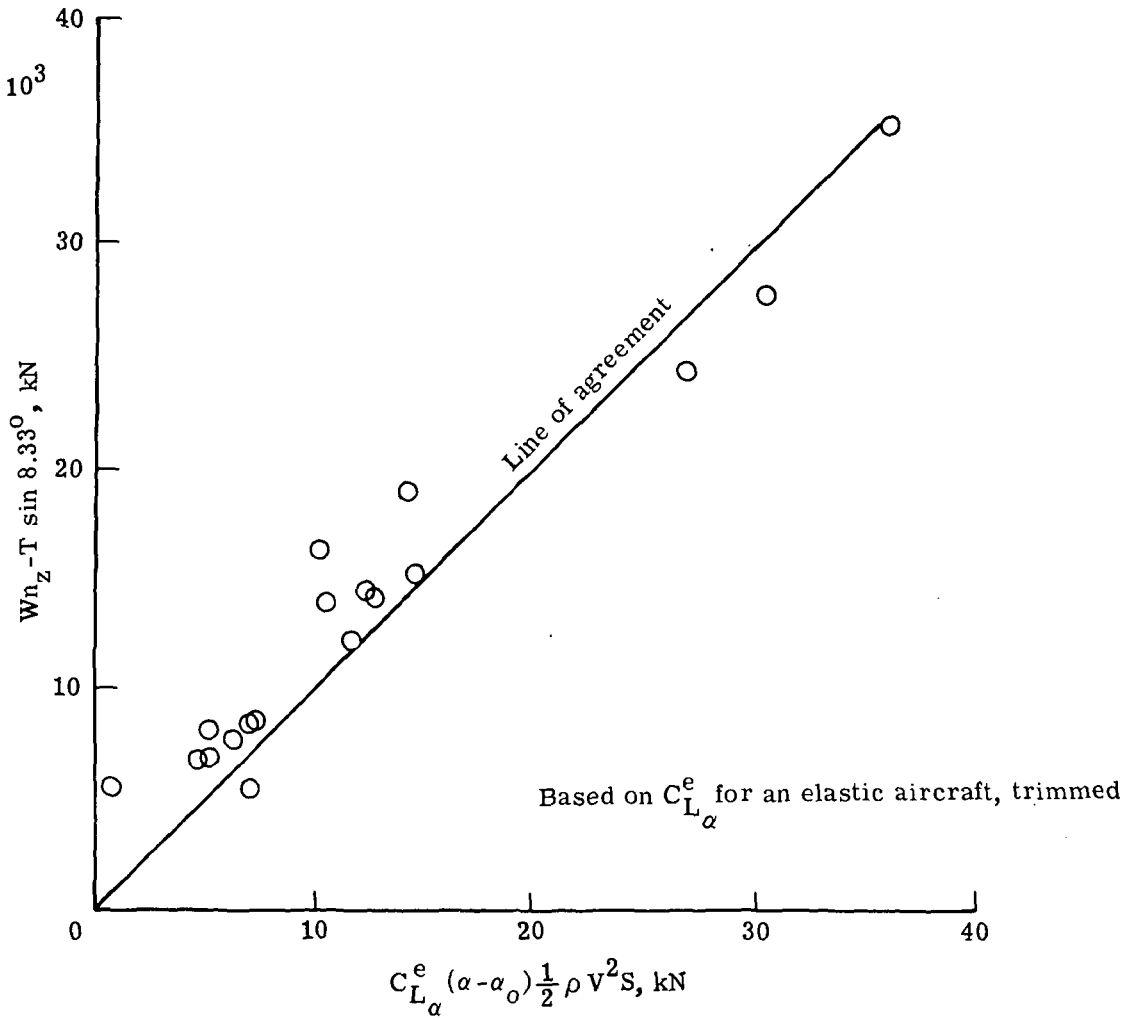

Figure 29.- Comparison of normal forces based on $C^e_{L_\alpha}$ for a trimmed elastic aircraft.

NATIONAL AERONAUTICS AND SPACE ADMINISTRATION
WASHINGTON, D.C. 20546

OFFICIAL BUSINESS
PENALTY FOR PRIVATE USE $300

SPECIAL FOURTH-CLASS RATE BOOK

POSTAGE AND FEES PAID
NATIONAL AERONAUTICS AND SPACE ADMINISTRATION
451

U.S.MAIL

POSTMASTER: If Undeliverable (Section 158 Postal Manual) Do Not Return

"The aeronautical and space activities of the United States shall be conducted so as to contribute . . . to the expansion of human knowledge of phenomena in the atmosphere and space. The Administration shall provide for the widest practicable and appropriate dissemination of information concerning its activities and the results thereof."

—NATIONAL AERONAUTICS AND SPACE ACT OF 1958

NASA SCIENTIFIC AND TECHNICAL PUBLICATIONS

TECHNICAL REPORTS: Scientific and technical information considered important, complete, and a lasting contribution to existing knowledge.

TECHNICAL NOTES: Information less broad in scope but nevertheless of importance as a contribution to existing knowledge.

TECHNICAL MEMORANDUMS: Information receiving limited distribution because of preliminary data, security classification, or other reasons. Also includes conference proceedings with either limited or unlimited distribution.

CONTRACTOR REPORTS: Scientific and technical information generated under a NASA contract or grant and considered an important contribution to existing knowledge.

TECHNICAL TRANSLATIONS: Information published in a foreign language considered to merit NASA distribution in English.

SPECIAL PUBLICATIONS: Information derived from or of value to NASA activities. Publications include final reports of major projects, monographs, data compilations, handbooks, sourcebooks, and special bibliographies.

TECHNOLOGY UTILIZATION PUBLICATIONS: Information on technology used by NASA that may be of particular interest in commercial and other non-aerospace applications. Publications include Tech Briefs, Technology Utilization Reports and Technology Surveys.

Details on the availability of these publications may be obtained from:

SCIENTIFIC AND TECHNICAL INFORMATION OFFICE

NATIONAL AERONAUTICS AND SPACE ADMINISTRATION

Washington, D.C. 20546